Pergamon

Tetrahedron: *Asymmetry* 10 (1999) 607–655

TETRAHEDRON: *ASYMMETRY*

TETRAHEDRON: ASYMMETRY REPORT NUMBER 41

Optical activity and stereochemistry of linear oligopyrroles and bile pigments †

Stefan E. Boiadjiev ‡ and David A. Lightner *

Department of Chemistry, University of Nevada, Reno, Nevada 89557, USA

Received 1 December 1998; accepted 14 January 1999

Contents

1. Introduction

Bile pigments belong to a class of pigments called linear tetrapyrroles,[1] although recent investigations of their stereochemistry suggest that most are not linear in shape.[1,2] Nonetheless, the term 'linear' satisfactorily distinguishes this class of oligopyrroles from those whose termini are covalently linked, as in the porphyrin macrocycles. Despite the fact that linear tetrapyrroles may assume many differing conformations, the linear representation seems to have been favored by Hans Fischer and is commonly found both in the literature and in texts.

* Corresponding author. E-mail: lightner@scs.unr.edu

† Dedicated to Professors Albert Moscowitz (deceased September 1996) and Francesc R. Trull (deceased June 1997).

‡ E-mail: stefcho@scs.unr.edu

PII: S0957-4166(99)00037-3

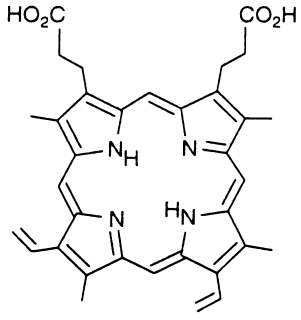

Protoporphyrin-IX

Linear oligopyrroles are widely found in nature, occurring during biosynthesis of cyclic tetrapyrroles and following their catabolism.[1] Bile pigments originate in porphyrin metabolism, usually by destruction of the iron complex of protoporphyrin-IX, called heme.[3] In mammals, an impressive array of bile pigments is produced (Fig. 1), including biliverdin and bilirubin and the fecal pigments arising from bacterial reduction of bilirubin in the gut: urobilin, stercobilin, etc.[4,5] In plants, the photoperiodicity pigment phytochrome, and the algal light-harvesting pigments phycoerythrin and phycocyanin all contain linear tetrapyrrole pigments related structurally to biliverdin and originate through protoporphyrin-IX.[1]

Cursory inspection of these pigments, derived from bilirubin and biliverdin, reveal the presence of stereogenic centers in and around the terminal lactam rings, suggesting the likelihood that these pigments might be found optically active from natural sources. Other, less obvious elements of stereochemistry concern the conformation of the pigments; and as it turns out, molecular conformation of bile pigments can have a dominating effect in their chiroptical measurements.

This was first shown by Moscowitz et al.[6] in their seminal study of the origin of optical activity in the urobilins, made almost 35 years ago without today's more sophisticated instrumentation and greater computational power. This study has, in our view, far wider implications and has profoundly influenced more recent stereochemical research in linear tetrapyrrole field. First, the authors pointed out that some linear tetrapyrroles, depending on their structure, were capable of exhibiting chiroptical phenomena originating not from the common one electron μ-m mechanism. Small alterations of structure, e.g., saturation of only one double bond, may lead to a switch from one optical activity mechanism to another — as will be seen in a comparison of biliverdin and bilirubin optical activity. Secondly, apparently for first time the importance of intramolecular hydrogen bonding was exquisitely and simply demonstrated as a conformation stabilizing force in the stereochemistry of tetrapyrroles. Naturally occurring linear tetrapyrroles bear up to 10 potential donor or acceptor sites for hydrogen bonding, and their mutual (intramolecular) interactions or interactions with the environment (intermolecular) are of the utmost importance for considerations of tetrapyrrole conformation.

In the following discussion of the optical activity of linear tetrapyrroles, we will refer to certain structural units found in them: (i) the dipyrrin (dipyrrylmethene or pyrromethene) chromophore of (blue-green) biliverdin and, especially, (red) urobilin and stercobilin, and (ii) the dipyrrinone (or pyrromethenone) chromophore found in (yellow-orange) bilirubin.

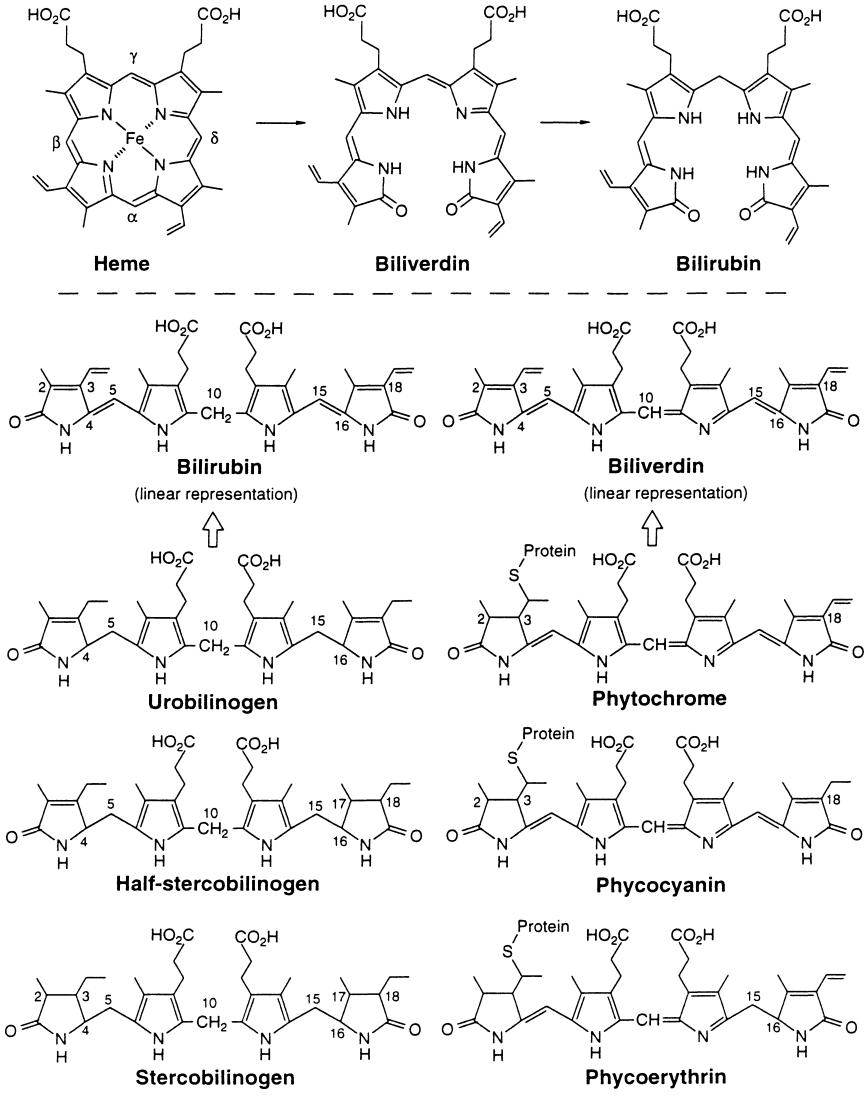

Figure 1. (Upper) Conversion of heme to biliverdin and bilirubin. (Lower left) Reduction of bilirubin to fecal bile pigment-chromogens: urobilinogen, half-stercobilinogen and stercobilinogen. The chromogens are easily oxidized at C(10) to give the corresponding red urobilin, half-stercobilin and stercobilin. (Lower right) Conversion of biliverdin to linear tetrapyrrole plant pigments

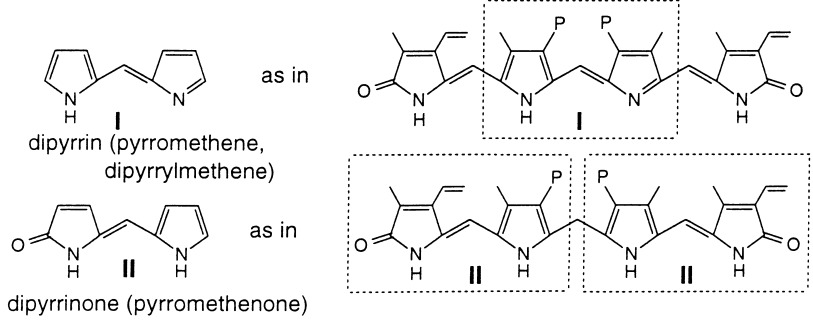

We start our review in a historical vein with one of the earliest observations of bile pigment optical activity, that of stercobilin in 1938. From there, we progress through explanations of the origin of its optical activity to the optical activity of biliverdins and phytochrome, and then to that of bilirubins. No attempt will be made here to render an exhaustive account of the natural optical activity of such pigments, or their optical activity induced by optically active solvents, additives, or complexing agents. The inclusion or exclusion of particular compounds is more a reflection of the authors' tastes and inclinations than it is of the importance of the subject matter to the field; the presence or absence of a particular reference is less indicative of its inherent worth than it is of the authors' narrowness or ignorance.

2. *l*-Stercobilin and *d*-urobilin

Heme, the red chromophore of hemoglobin and cytochromes, is metabolized in nature to produce an array of linear tetrapyrrolic compounds with fascinating stereochemistry and chiroptical properties (Fig. 1). Following oxidative cleavage of the protoporphyrin-IX macrocycle, typically at the α-bridge, a series of reduction processes follow in mammalian metabolism.[3–5] Bile pigments formed at the end of the reduction chain are stercobilinogen and urobilinogen, which upon air oxidation are converted into stercobilin-IXα (stercobilin, **1**, 2,3,17,18-tetrahydrourobilin) and mesourobilin-IXα (urobilin, **2**).[7]

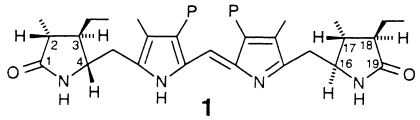

1

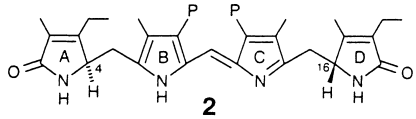

2

The urobilinoid pigment found in human faeces, natural (−)-stercobilin (**1**), was first obtained in crystalline form by C. J. Watson in 1932.[8] The optical activity of (−)-stercobilin[9] and (+)-urobilin (**2**)[10] was recognized shortly thereafter. Both natural bile pigments are characterized by extremely high specific rotations of their hydrochlorides in chloroform: $[\alpha]_D$ −4000 for stercobilin and $[\alpha]_D$ +5000 for urobilin.[11] The corresponding free bases retain the sign of $[\alpha]_D$ but have only about 20% of these values.[11] (Their hydrogenated derivatives (chromogens, Fig. 1) exhibited much lower specific rotations.)[12] These very large optical rotation values at the sodium D-line (589 nm) of these red-colored pigments are (in part) a consequence of the strong absorption band (~490 nm) of their dipyrrin (**I**) chromophores.

The first optical rotatory dispersion (ORD; for a full list of abbreviations see Appendix A) measurement of bile pigments: (−)-**1** and (+)-**2** (as hydrochlorides in $CHCl_3$) in the region 620–470 nm was reported by Gray, Jones, Klyne and Nicholson in 1959.[13] (−)-Stercobilin showed a strong negative Cotton effect (CE), and (+)-urobilin a strong positive CE corresponding to the visible range absorption band centered near 490 nm. Thus, the pigments exhibited mirror image ORD curves but the amplitude A (difference in molecular rotation [M] at the peak and trough of the ORD curve) of (+)-**2** which contains vinylogous substituents at the C(4) and C(16) chiral centers was much greater ($A\sim +300\times10^3$) than that of (−)-**1** ($A\sim -130\times10^3$) which has aliphatic substituents.[13]

In 1964, Moscowitz and coworkers rationalized the extremely large optical rotations and ORD amplitudes of (−)-stercobilin (Fig. 2) and (+)-urobilin.[6] Based on a theoretical treatment of chiroptical phenomena[14] the authors related the natural pigments' chromophore to an inherently dissymmetric dipyrrin chromophore as opposed to more often encountered cases of inherently symmetric, but dissymmetrically perturbed chromophore.[15] The rotational strengths[14,16] associated with an inherently dissymmetric chromophore are usually one order or more orders of magnitude ($R\sim10^{-38}$ cgs) greater than those associated with inherently symmetric but dissymmetrically perturbed chromophores. From

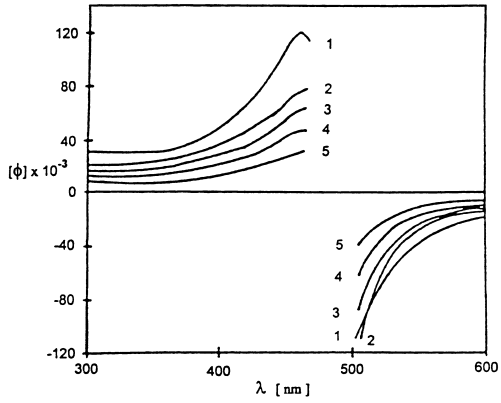

Figure 2. ORD curves of *l*-stercobilin·HCl in chloroform:methanol (0.001 ml concentrated HCl per ml of methanol added to preserve the hydrochloride). The percent (v/v) methanol was: Spectrum 1, 0; Spectrum 2, 25; Spectrum 3, 50; Spectrum 4, 75; Spectrum 5, 100

first[13] and subsequent[6] ORD measurements, the rotational strengths for (−)-**1** and (+)-**2** were estimated to be R∼10^{-38} cgs, characteristic of an inherently dissymmetric chromophore. To account for the intensity, Moscowitz et al.[6,16] suggested a twisted dipyrrylmethene (dipyrrin) unit (**I**) of fixed helicity and stabilized by a network of four intramolecular hydrogen bonds, as shown in Fig. 3 for urobilin. However, the sense (or handedness) of the helical twist (*M* or *P*) could not be determined directly from the sign of the rotation or CE. The relative configuration at the C(4) and C(16) stereogenic centers was suggested by inspection of space-filling (Stuart–Briegleb) molecular models, which show that the sense of twist of the dipyrrin chromophore associated with an (*S*,*S*) absolute configuration was of opposite helicity to that associated with the (*R*,*R*) configuration. Hence the intense CEs corresponding to the (*S*,*S*) and (*R*,*R*) stereochemistries are predicted to be oppositely signed. Since a given helicity is determined by intramolecular hydrogen bonding, (−)-stercobilin should have either the (*S*,*S*) or (*R*,*R*) absolute configuration, but not (*S*,*R*) or (*R*,*S*). In the latter, steric constraints dictated by configurations at C(4) and C(16) do not permit the full complement of intramolecular hydrogen bonds enjoyed with the (*R*,*R*) and (*S*,*S*) configurations. Thus, the (*R*,*S*) and (*S*,*R*) diastereomers can fold into half intramolecularly hydrogen-bonded *P*- and *M*-helical conformations with equal facility, with the result that they would be almost equally populated and the optical activity very low. The authors[6,16] thus inferred that if (−)-**1** had the (*S*,*S*) configuration, then (+)-**2** must have (*R*,*R*) configuration. Seven years later, confirmation of the absolute configuration of (−)-**1** came from degradation studies, but more than 30 years passed before an unequivocal assignment of absolute configuration by X-ray crystallographic analysis and synthesis was realized, vide infra.

Experimental support of the hypothesis for a twisted and intramolecularly hydrogen-bonded central core in **1** and **2** was found by titration of chloroform solutions of (−)-**1**·HCl and (+)-**2**·HCl with methanol, trifluoro- or trichloroacetic acid.[6,16] This resulted in a significant large and reversible decrease in optical activity as measured by ORD (Figs. 2 and 4) and ascribed to the disruption of intramolecular hydrogen bonding so essential for maintaining the *M*- or *P*-helicity of the dipyrrylmethene chromophore. The estimated rotational strength dropped to R∼10^{-40} cgs, a value more characteristic of an inherently symmetric chromophore. These bile pigments thus provided a very nice illustration of an inherently dissymmetric chromophore and its racemization, depending upon solvent polarity and its hydrogen-bonding ability.

The foregoing analysis also provides an explanation for the weak optical activity of hydrogenated urobilin derivatives[12] to give the chromogens, stercobilinogen and urobilinogen (Fig. 1). Hydrogenation

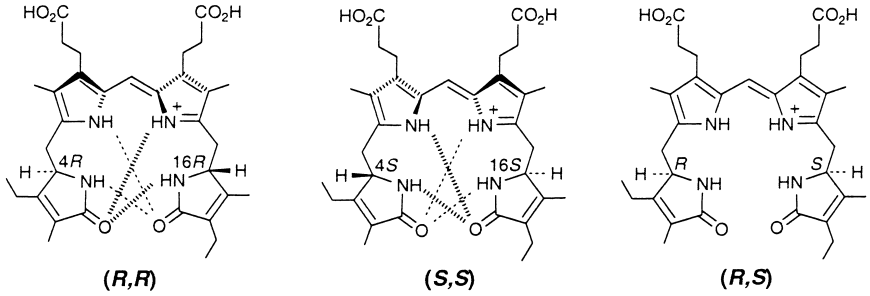

Figure 3. Intramolecular hydrogen-bonded urobilin hydrochloride. The 'linear' tetrapyrrole folds into a porphyrin-like shape in order to allow the lactam carbonyls to participate in hydrogen bonding to the opposing NHs, and the configuration at C(4) and C(16) determine the dipyrrin helicity: *M* for (4*R*,16*R*); *P* for (4*S*,16*S*)

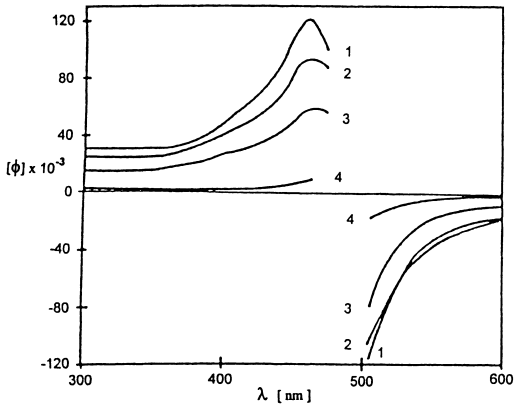

Figure 4. ORD curves for titration of *l*-stercobilin·HCl in $CHCl_3$ with TFA. The mole ratio of TFA to *l*-stercobilin·HCl, was: Spectrum 1, 0; Spectrum 2, 50; Spectrum 3, 800; Spectrum 4, 5000

of the dipyrrin chromophore destroys the conjugated twisted π-electron system involving the two central rings B and C, thereby eliminating the possibility of achieving an inherently dissymmetric conjugated chromophore, irrespective of any intramolecular hydrogen bonding.

A strong decrease in optical activity, measured by the rotation at 589 nm of (+)-urobilin was observed upon titration with zinc ions, reaching a plateau after addition of 2 equiv. of Zn^{2+}.[17] Similar titration of (−)-stercobilin showed a more complex behavior at low Zn^{2+} concentration, and sign reversal with low rotation at high Zn^{2+} concentration. The ORD curves from solutions of (−)-**1** and (+)-**2** containing zinc ions were also measured and found to follow the same trend: diminished Cotton effects.[17] Although not isolated and characterized, formation of zinc (and copper) complexes of (−)-**1** and (+)-**2** was proposed, with structures involving pigments' lactim tautomer in a porphyrin-like conformation. Such conformations should lead to planarization of the formerly twisted dipyrrin chromophore and a concomitant decrease of optical activity.

The first CD spectra of (−)-**1** [$\Delta\varepsilon_{489}^{max}$ −36 ($CHCl_3$)] and (+)-**2** [$\Delta\varepsilon_{492}^{max}$ +40 ($CHCl_3$)] and their temperature dependence were reported in 1970 by Lightner, Docks, Horwitz and Moscowitz.[18] In chloroform at low temperatures, the long wavelength 490 nm CE signs remained invariant, and the rotatory strength even increased. In contrast, in methanol:glycerol (9:1) at low temperatures, the CE underwent sign reversal in both compounds (Fig. 5). The inverted low temperature 490 nm CEs also had large rotational strengths, implying reversal of the handedness of the twisted dipyrrin chromophore. Based on an examination of space-filled molecular models, the authors proposed that the dipyrrin chromophore was twisted into a left-handed (*M*) helix when the C(4) and C(16) stereogenic centers

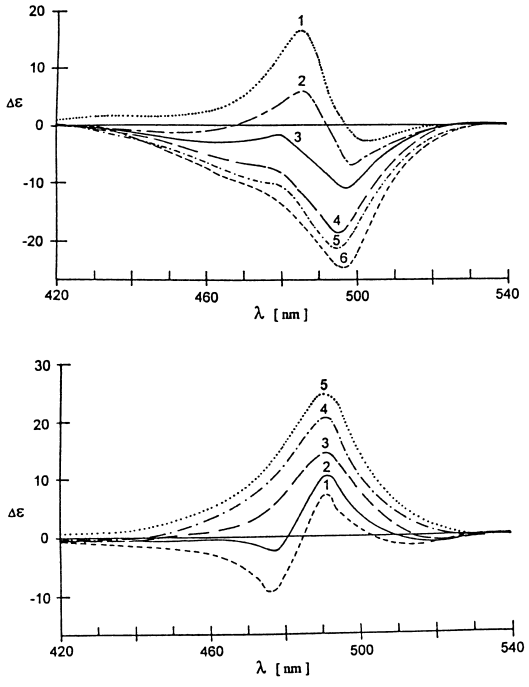

Figure 5. Temperature-dependent CD curves of *l*-stercobilin·HCl (upper, Spectrum 1, 163 K; Spectrum 2, 188 K; Spectrum 3, 216 K; Spectrum 4, 253 K; Spectrum 5, 272 K; Spectrum 6, 297 K) and *d*-urobilin·HCl (lower, Spectrum 1, 163 K; Spectrum 2, 198 K; Spectrum 3, 232 K; Spectrum 4, 262 K; Spectrum 5, 296 K) in methanol:glycerol 9:1 (v/v)

possessed the (*R*,*R*) absolute configuration and into a right-handed (*P*) helix for (*S*,*S*) configuration. In polar and hydrogen-bonding solvents such as methanol:glycerol, the four intramolecular hydrogen bonds[6,16] are partially disrupted, and an equilibrium between intramolecularly H-bonded coiled and uncoiled (or at least more open) form occurs. In the uncoiled conformations the dipyrrin chromophore is not constrained to single homochiral geometry, and both *M*- and *P*-helicities may occur. At room temperature, the uncoiled forms contribute little to the net optical activity due to cancellation of contributions from the nearly equally populated *M*- and *P*-helical conformers. At lower temperatures, however, the population difference increases, and significant optical activity is evinced by the uncoiled forms, responsible for CD sign reversal. In nonpolar solvents that do not interfere with intramolecular hydrogen bonds, such as $CHCl_3$, the coiled forms, without helicity change, dominate the equilibrium at all temperatures studied. The solvent and temperature dependent conformational mobility revealed from CD spectroscopy by this study[18] hints that synthetic model linear tetrapyrroles in a typical organic solvent might have a conformation considerably altered from that of a structurally very similar native analog in aqueous environment, in vivo, under certain circumstances.

3. Absolute configuration of the urobilins

Traditionally, total synthesis of a natural product is considered to be the definitive, rigorous proof of its structure, including absolute configuration. Plieninger and Lerch first synthesized racemic stercobilin,[19] and subsequently Plieninger and Ruppert undertook the challenging task (six chiral centers) of synthesizing natural stercobilin,[20] which would determine its absolute configuration. The synthetic plan involved coupling two different dipyrroles, one optically active, the other racemic. This elegant approach entailed

only one optical resolution step (a dipyrrole) and took advantage of the fact that its subsequent coupling with the second racemic dipyrrole gave diastereomers which were readily separated. Racemic 2,3-*trans*-3,4-*cis* diacid **3** (only the relative configurations were then known) was resolved by recrystallization of its brucine salts from CH_3OH to afford (+)-**3** in higher ee. Thermal decarboxylation gave the important optically active dipyrrole-dihydroisoneobilirubic acid **4**. Its (−)-enantiomer was reacted with racemic 2,3-*trans*-3,4-*cis* aldehyde **5** in the presence of acid (Scheme 1). The resulting diastereomeric stercobilins were separated by recrystallization, and a strongly negatively rotating isomer (**6**) was obtained in a pure state. The other 'quasi-*meso*' isomer **7**, presumably with low optical rotation, was not isolated and characterized. Similarly, condensation of (−)-**4** with racemic 2,3-*trans*-3,4-*trans* aldehyde (**8**) gave one strongly negatively rotating stercobilin isomer (**9**) and a 'quasi-*meso*' isomer (**10**) (not isolated), as in Scheme 2. The dextrorotatory stercobilin-IXα isomer corresponding to **6** was also obtained reacting (+)-**4** with **5**.

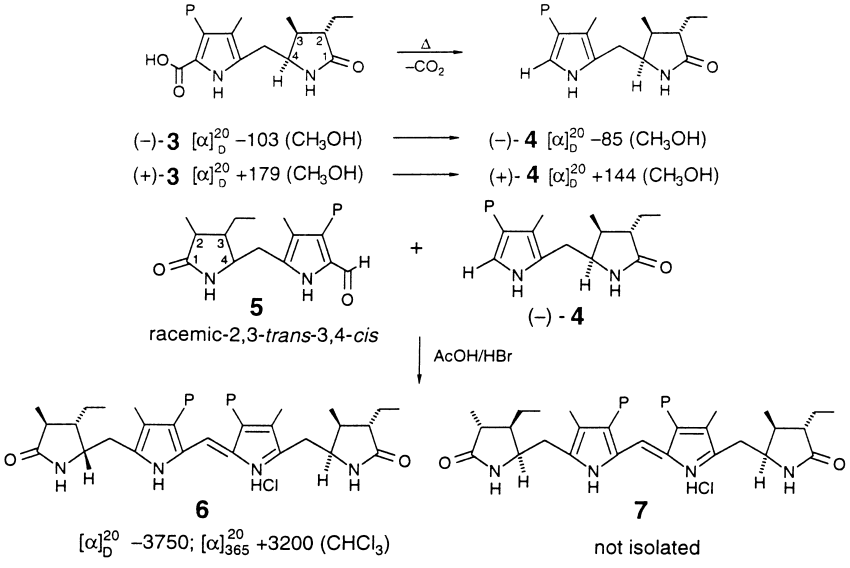

Scheme 1.

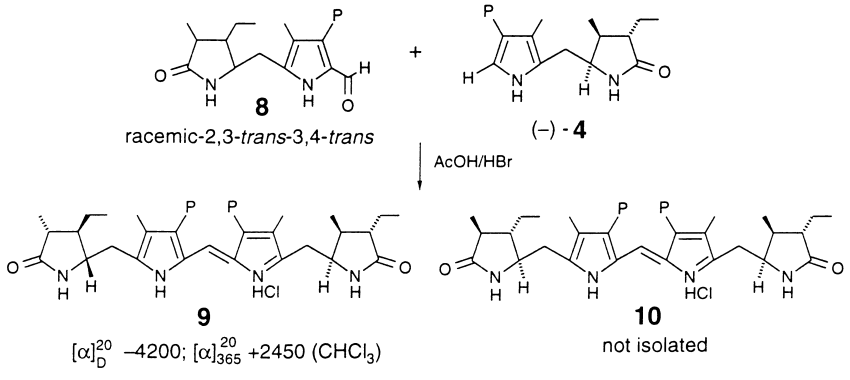

Scheme 2.

From their UV–vis and IR spectra, and by comparison from TLC both levorotatory stercobilins **6** and **9** were undistinguishable from the natural (−)-**1**. The Debye–Scherrer X-ray diagram of **6** proved to be the same as that of (−)-**1**, and at this point it appeared that the natural product was indeed obtained synthetically.[20] However, differences in the formation of the $FeCl_3$ complex of (−)-**1** and (−)-**6** were

found, and this prompted further study, including a comparison of the degradation products obtained by chromic acid oxidation. As it turned out, this chemical correlation, in conjunction with chiroptical spectroscopy was crucial in determining the absolute configuration of (−)-stercobilin **1**.[21] Chromic acid degradation of (−)-**3**, the synthetic precursor of **6** and **9**, afforded (−)-(2*S*)-methyl-(3*S*)-ethylsuccinimide (**11**). Similar degradation of natural (−)-**1** gave a high yield and ee of *ent*-**11**, the (+)-(2*R*,3*R*) enantiomer. Comparison of (−)-**11** and (+)-**11** by CD spectroscopy showed a clear mirror image relation, consequently (−)-**1** and (−)-**6** were not identical. ^{1}H-NMR analysis pointed to the *trans*,*trans* stereochemistry of the C(3)/C(4) and C(16)/C(17) hydrogens while in **6** it was *cis*,*cis*. Combining all of the information, it was concluded that the natural (−)-stercobilin **1** has (2*R*,3*R*,4*S*,16*S*,17*R*,18*R*) absolute configuration.[21] Consequently, it is the (4*S*,16*S*) configuration in (−)-**1** that is responsible for the chiral twist of dipyrrin chromophore **I** associated with strong negative CE near 490 nm.

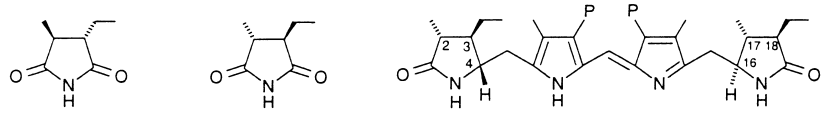

Self-condensation of (−)-**4** or (+)-**4** in presence of triethylorthoformate/HBr afforded the symmetrically substituted stercobilin-IIIα hydrochloride (**12**) (Scheme 3) with large negative and positive rotation at 589 mn, respectively.[20]

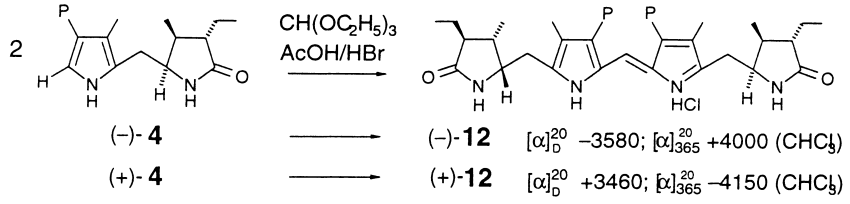

Scheme 3.

Racemic acids **13** and **16** were resolved via their quinine salts to afford (+)-**13** and (+)-**16**, which were thermally decarboxylated to yield (+)-**14** and (+)-**17**, respectively, or esterified to give (+)-**15** and (+)-**18**, respectively.[22] The symmetrically substituted (+)-mesourobilin-XIIIα hydrochloride (**19**) and (+)-mesourobilin-IIIα hydrochloride (**20**) were prepared by self-condensation of (+)-**14** and (+)-**17**, respectively, in the presence of triethylorthoformate/HBr, as shown in Scheme 4. Condensation of (+)-**14** or (−)-**14** with racemic aldehyde **21** led to the unsymmetrically substituted (+)-mesourobilin-IXα hydrochloride [(+)-**22** or (−)-**22**, respectively], as in Scheme 5, leaving behind a more soluble 'quasi-*meso*' product. All mesourobilins **19**, **20**, **22** exhibited extremely high optical rotation. Their absolute configuration, however, was not known at the time of this work.[22]

Earlier reports that natural (+)-urobilin contains an 18-vinyl substituent[7] stimulated Gossauer and Weller[23] to undertake its synthesis. They followed the previously mentioned route,[22] as outlined in Scheme 6. Acid catalyzed coupling of optically active (+)-**13** with racemic aldehyde **23**, followed by treatment with diazomethane, yielded a mixture of diastereomeric (18-vinyl)mesourobilins-IXα dimethyl esters, which were separated chromatographically and converted into hydrochlorides **24** and **25**. Diastereomer **24** exhibited a very large positive optical rotation and strong CD CEs: $\Delta\varepsilon^{max}_{495}$ +35.8, $\Delta\varepsilon^{max}_{235}$ −23.4 (CH_2Cl_2) and was assigned (4*R*,16*R*) absolute configuration, (cf. Brockmann et al.[21] and Plieninger et al.[22]). The 'quasi-*meso*' diastereomer (−)-**25** with a much lower rotation and weaker CD: $\Delta\varepsilon^{max}_{520}$ −0.56, $\Delta\varepsilon^{max}_{487}$ +0.17, $\Delta\varepsilon^{max}_{455}$ −0.75, $\Delta\varepsilon^{max}_{330}$ +1.12, $\Delta\varepsilon^{max}_{255}$ +5.22 (CH_2Cl_2) was assigned the (4*R*,16*S*) absolute configuration.[23] However, even at this date (1978), the configuration was indirectly deduced from chiroptical data and based on Moscowitz's twisted dipyrrin chromophore hypothesis,[6,16] vide supra.

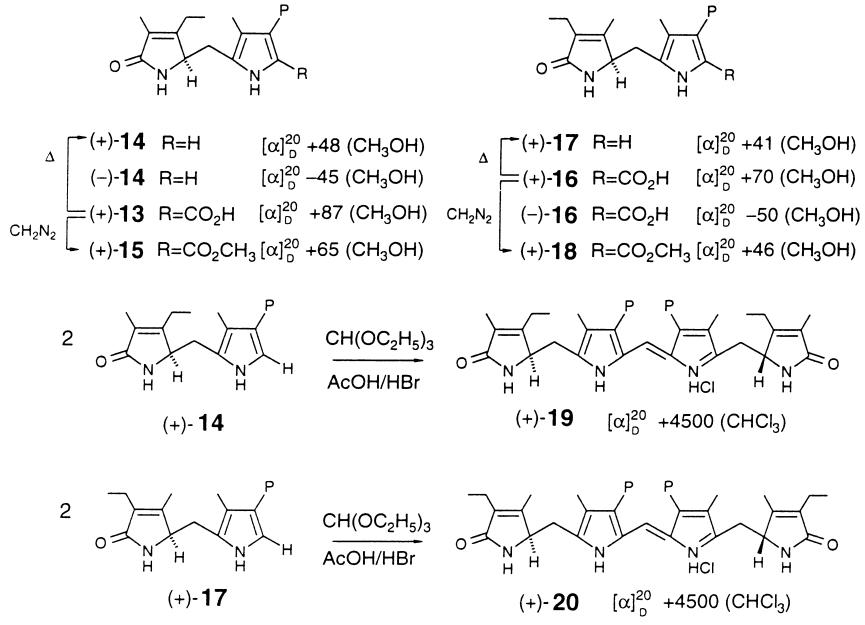

Scheme 4.

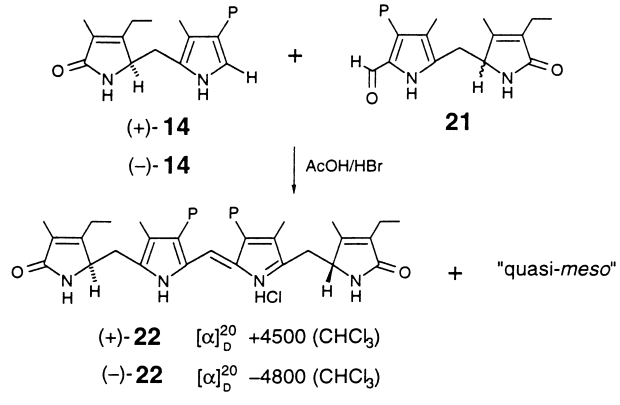

Scheme 5.

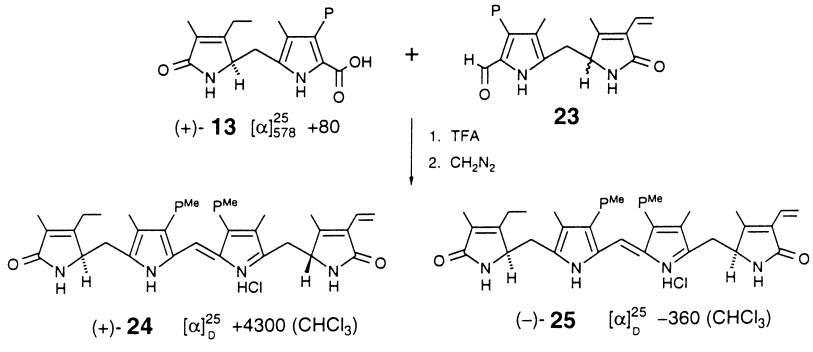

Scheme 6.

In 1987 Gossauer et al. presented the first unequivocal assignment of the absolute configuration of an urobilin-IIIα type model bile pigment **31**.[24] The authors' repeated attempts to obtain crystals of (+)-mesourobilin-IXα and (+)-mesourobilin-IIIα or their synthetic precursors suitable for X-ray crystallography had failed. So, they envisaged C_2-symmetric urobilin **31** as an appropriate model compound, where the lack of flexible C(8),C(12)-propionic acids would entropically favor crystallization. The breakthrough, however, came at an earlier stage, at the precursor: 1,4,5,10-tetrahydro-1-oxodipyrrin-9-carboxylic acid (**26**). Complete optical resolution of racemic acid **26** was achieved by fractional recrystallization of its strychnine salt from CH_3OH. The absolute configuration was determined to be (4*R*) for the dextrorotatory acid *ent*-**26** (enantiomeric of that shown below) using X-ray crystallographic analysis of its amide (*ent*-**30**) formed with (−)-(*S*)-1-(1-naphthyl)ethylamine. The absolute configuration (4*S*) of (−)-**26** was reconfirmed recently by X-ray structure analysis of (−)-**30**.[25] The absolute configuration of (−)-(4*S*)-aldehyde **27** follows from chemical correlation with (−)-**26**. Acid catalyzed condensation of enantiomerically pure (−)-**26** and (−)-**27**, both with firmly determined absolute configuration gave (−)-(4*S*,16*S*)-8,12-bis[de(2-carboxyethyl)]mesourobilin-IIIα hydrochloride (**31**), as shown in Scheme 7. This model urobilin exhibited a strong negative rotation and CD CE ($[\alpha]_D^{20}$ −5000 (*c* 7.0×10^{-4}, $CHCl_3$) and $\Delta\varepsilon_{499}^{max}$ −53 ($CHCl_3$)). The latter increased to $\Delta\varepsilon_{499}^{max}$ −67.5 at 238 K (Fig. 6). Thus, Gossauer et al.[24] proved that the (4*S*,16*S*) urobilin displays a negative CD Cotton effect for its visible absorption band. The strong negative CE of (−)-**31** is also in agreement with the tentative assignment (4*R*,16*R*) for the configuration of (+)-mesourobilin-IXα.[21]

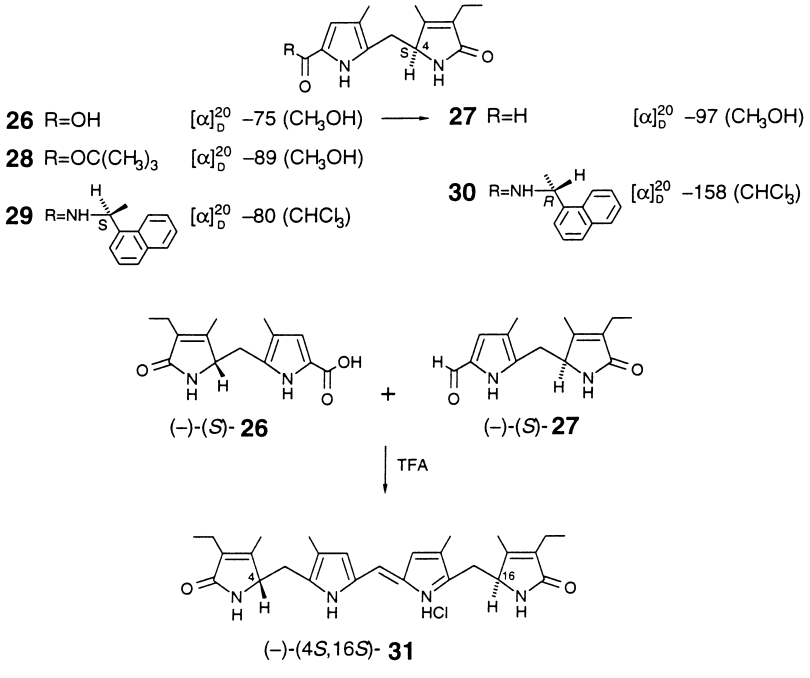

Scheme 7.

It should be noted here that the three-way relation between the C(4), C(16) absolute configuration, the CD CE, and the dipyrrin **I** chromophore helicity in urobilins has not yet been firmly verified by experiment. X-Ray diffraction analysis of the synthetic precursor *ent*-**30** established experimentally only the relationship between the (4*S*,16*S*) absolute configuration of urobilins and their negative CD Cotton effect sign. The sense of twist of an inherently chiral dipyrrin chromophore, however, cannot be established from the data above. Lightner et al.[18] postulated that right-handed (*P*-helicity) is conditioned

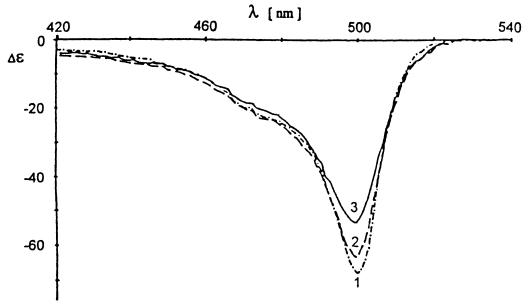

Figure 6. Temperature-dependent CD curves of (−)-(4*S*,16*S*)-8,12-bis[de(2-carboxyethyl)]mesourobilin-IIIα hydrochloride (**31**) ($CHCl_3$, c=1.47×10^{-5} M). Spectrum 1, 238 K; Spectrum 2, 268 K; Spectrum 3, 298 K. Redrawn from Pasquier et al.[24]

by (4*S*,16*S*) configuration, and if correct, a right-handed helical π-twisted system is to be associated with a negative CE, which is opposite to that found in hexahelicene.[26]

The optically pure urobilin model compound **37** was recently synthesized.[27] Hydrogens at chiral centers C(4) and C(16) are replaced by methyl groups to prevent facile racemization. The (4*R*,16*R*) absolute configuration of (+)-**37** follows from that of its building blocks precursors (−)-**35** and (−)-**36** (Scheme 8). Both enantiomerically pure (−)-**35** and (−)-**36** were prepared starting from racemic hydroxamic acid **32**, which was completely resolved into individual enantiomers by fractional recrystallization of the diastereomeric carbamates formed from (+)-(*S*)-1-(1-naphthyl)ethyl isocyanate. Homochiral carbamate (−)-**33** was transesterified with CH_3OH to afford (−)-**32**, whose absolute configuration was determined to be (4*R*) by X-ray crystallographic analysis of the corresponding (−)-camphor-10-sulfonate (**34**). The unknown C(4) absolute stereochemistry of **32** was thus related to the known configuration of the camphor skeleton. Enantiomerically pure (−)-**32** was converted into the corresponding dipyrrin-1(10*H*)-one derivative, (−)-**35**, by treatment with aqueous $TiCl_4$ in AcOH/THF. Its pyrrole α-*tert*-butyl ester was deprotected, and after one pot decarboxylation it was formylated in situ to afford (−)-**36**. Thus, both levorotatory **35** and **36** were shown to have the (4*R*) configuration and therefore their product (**37**) has the (4*R*,16*R*) configuration.

The free base of (+)-**37** was more stable than usual urobilins bearing tertiary chiral centers, and showed $[\alpha]_D^{20}$ +1960 (c 4.8×10^{-3}, CH_2Cl_2) and CD: $\Delta\varepsilon_{469}^{max}$ +18.2 (CH_3OH), $\Delta\varepsilon_{465}^{max}$ +17.0 (CH_2Cl_2). In contrast, the hydrochloride of (4*R*,16*R*)-**37** had $[\alpha]_D^{20}$ +4900 (c 1.4×10^{-3}, CH_2Cl_2) and $\Delta\varepsilon_{496}^{max}$ +69.0 (CH_2Cl_2). The extremely large positive CE is in agreement with the positive Δε found for natural (+)-(4*R*,16*R*)-urobilin (**2**). This result supported the relationship between chiroptical properties and absolute configuration of the chiral C(4), C(16) atoms even though methyl groups rather than H atoms are present on both chiral centers in **37**.[27]

However, a possible ambiguity arises from the fact that the C(4)/C(16) hydrogens in (+)-**2** have a lesser steric demand, than the C(4)/C(16) methyls of (+)-**37**, relative to the C(5)/C(15) methylenes. Yet winding of the helical chromophores of (+)-2 and (+)-**37** appears the same. The helical twist (*M* or *P*) of the inherently dissymmetric dipyrrin chromophore again cannot be inferred from these experimental results. It was noted that both (−)-**28**, $\Delta\varepsilon_{282}^{max}$ −7.1 (CH_3OH), and (−)-**35**, $\Delta\varepsilon_{285}^{max}$ −5.8 (CH_3OH), had the same CD CE sign, despite the fact that the absolute configuration at C(4) is opposite.[25] As they differ mainly in the substituents on the lactam ring, a similar preferred conformation is probably determined in both cases, following from steric interactions of these substituents with the pyrrole ring rather than by intramolecular hydrogen bonding.

In order to shed more light on the relation between CD, configuration and conformation of urobilin-like molecules, Gossauer et al. recently reported on the properties of optically active difluoroboron

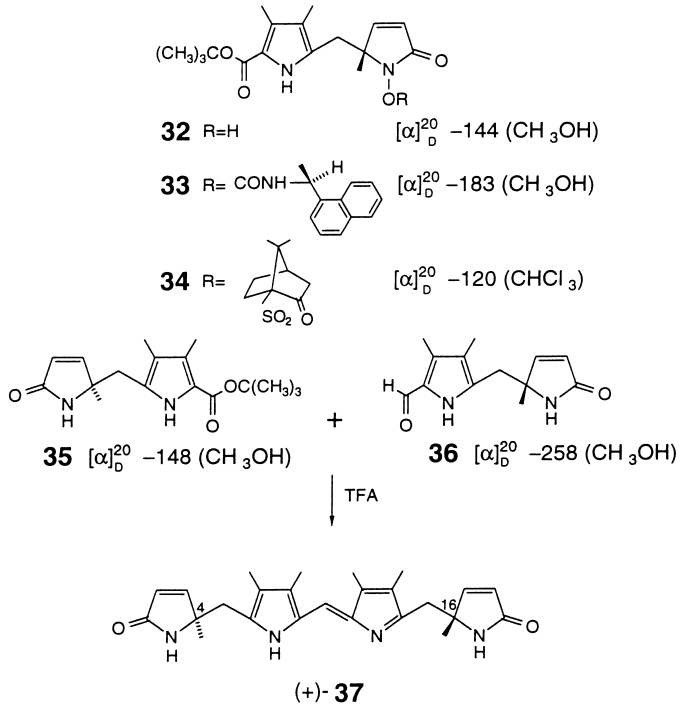

Scheme 8.

complexes **38** and **39A**,**B**, obtained from homochiral **31** and **37**, respectively (Scheme 9).[25] BF_2 complex **38** exhibited a smaller optical rotation and CD (Fig. 7) than (presumably helical) **31**: for **38** in CH_2Cl_2, $\Delta\varepsilon_{545}^{max}$ −9.70 (293 K) increases to $\Delta\varepsilon_{545}^{max}$ −11.4 (253 K); in DMF $\Delta\varepsilon_{546}^{max}$ −7.98 (293 K) increases to $\Delta\varepsilon_{546}^{max}$ −10.9 (253 K). From the very small temperature dependence of the CD of **38**, an equilibrium involving antipodal helicities[18] was excluded. Extensive $^1H\{^1H\}$ NOE experiments on **38** in both CD_2Cl_2 and DMF-d_7 (important NOE enhancements are shown on the structures as curved arrows in Scheme 9) pointed to an anticlinal conformation around the C(4)–C(5) and C(15)–C(16) bonds. Thus, the BF_2 chelate appears to adopt a 'stretched' 9*Z*, 4(5)−*ac*, 5(6)−*sc*, 10(11)*sp*, 14(15)−*sc*, 15(16)−*ac* conformation in both DMF and CH_2Cl_2. The situation for the BF_2 complex of **37** was much more complicated, and the authors considered two distinct conformers **39A** and **39B**.[25] Oppositely signed rotation and CD CEs were observed in CH_2Cl_2 and DMF (Fig. 7); in CH_2Cl_2, $\Delta\varepsilon_{538}^{max}$ +67.2 (293 K) increases to $\Delta\varepsilon_{538}^{max}$ +82.1 (253 K); in DMF, $\Delta\varepsilon_{535}^{max}$ −29.5 (293 K) increases to $\Delta\varepsilon_{535}^{max}$ −48.1 (253 K). The variable temperature CD intensities behaved as a linear function of inverse temperature in DMF, and as binomial function in CH_2Cl_2. This was taken to indicate the presence of conformers of comparable entropy in DMF, and higher entropy difference conformers in CH_2Cl_2, presumably **39A** and **39B**. The reason for the striking contrast in the behavior of **38** and **39** is the presence of methyl groups at C(4)/C(16) in the latter. In the BF_2 chelate of **37**, an extended conformation analogous to **38** is less favorable due to steric repulsion between the C(4)/C(16) methyls and the methyl groups on C(7) and C(13). Indeed, in both **39A** and **39B** conformers, in DMF-d_7 and CD_2Cl_2, respectively, the C(4)/C(16) methyls were found to lie in a gauche arrangement to both the pro-*R* and pro-*S* hydrogens of C(5)/C(15) methylene groups. The preferred conformation in DMF extracted from $^1H\{^1H\}$ NOE experiments was **39A**: 9*Z*, 4(5)−*sc*, 5(6)−*sp*, 10(11)*sp*, 14(15)−*sp*, 15(16)−*sc*; and in CH_2Cl_2 it is **39B**: 9*Z*, 4(5)−*sc*, 5(6)+*sc*, 10(11)*sp*, 14(15)+*sc*, 15(16)−*sc*. Titrating a CD_2Cl_2 solution of **39B** with DMF-d_7 promoted conformational conversion into **39A** as observed in the ^1H-NMR by a swap of the C(5)/C(15) AB proton chemical shifts via a cross-over point. Only

the BF_2 complex **39B** in CD_2Cl_2 showed ^1H–^{19}F through space spin–spin coupling between BF_2 and lactam NHs consistent with stabilization of **39B** conformer by intramolecular NH···F hydrogen bonding. Surprisingly, an X-ray crystallographic analysis of samples of **39** obtained from DMF/Et_2O and from $CHCl_3$/hexane (expected **39B**) revealed identical structures in the solid state — corresponding to **39A**.[25] This result emphasized the relevance of conformational analysis in solution, not only solid state data, when explaining chiroptical phenomena. The authors[25] abandoned the concept that the CD originates from a twisted dipyrrin chromophore because the crystal structure showed a planar boron–dipyrrin moiety. It is not clear, however, whether it remains planar in solution. A sector rule was proposed, similar to many others for inherently symmetric but dissymmetrically perturbed chromophores, relating the observed CD sign with the extrachromophoric geometry (second chiral sphere according to Snatzke[28]). Yet, the observed rotatory strengths of **38**–**39A**,**B** are at least one order of magnitude higher than those of (inherently dissymmetric) skewed α,β-unsaturated ketones.[29]

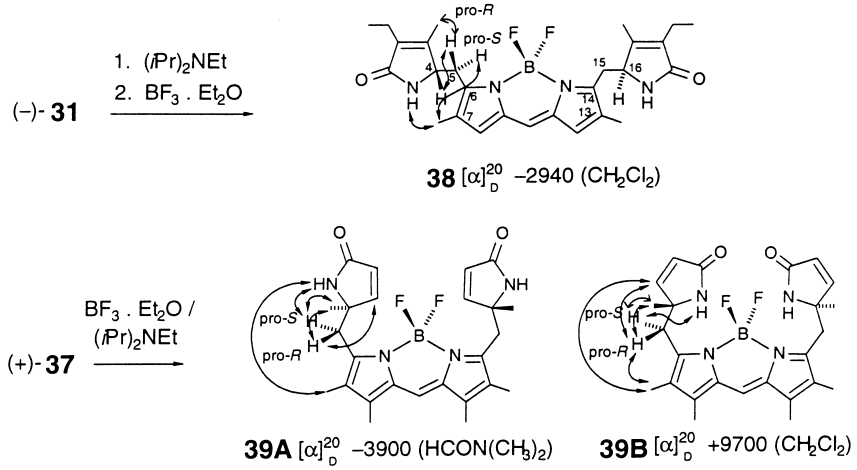

Scheme 9.

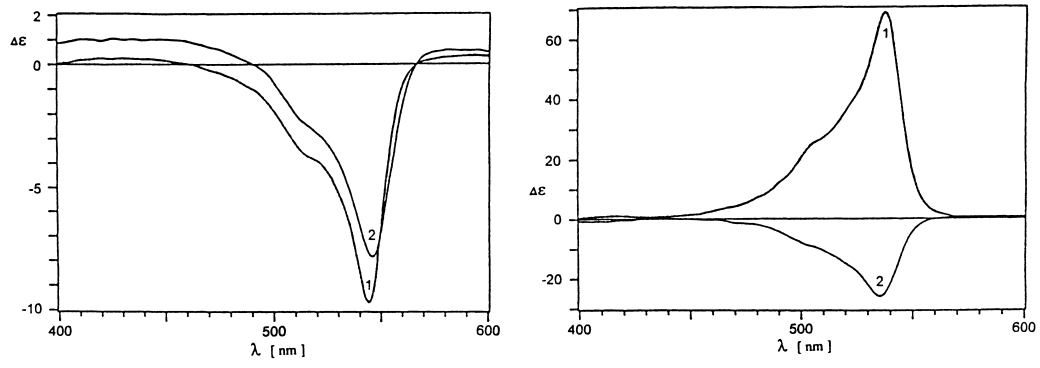

Figure 7. Circular dichroism spectra of difluoroboron complexes: upper, **38** in CH_2Cl_2 (Spectrum 1) and DMF (Spectrum 2) solutions; lower, **39B** in CH_2Cl_2 (Spectrum 1) and **39A** in DMF (Spectrum 2) solutions. Redrawn from Gossauer et al.[25]

4. Biliverdins: esters and amides

The dipyrrin moiety (**I**) is present in the central B and C rings of the 1,19-dioxobilin skeleton. Biliverdin-IXα (biliverdin, **40**) is one of the most important members of this large family of linear tetrapyrroles and is formed from heme by regioselective α-oxidation through the action of the enzyme heme oxygenase (Fig. 1). In the plant kingdom, 1,19-dioxobilins are also found, e.g., in red algae. Until 1976, when Sheldrick published an X-ray crystallographic study on biliverdin dimethyl ester,[30] no other firm data on the 1,19-dioxobilin chromophore geometry in crystalline state were available. Since then a wealth of X-ray crystallographic data has accumulated.[1] The data indicate a helical chromophore geometry. In (4*Z*,10*Z*,15*Z*)-5,9,14-synperiplanar etiobiliverdin-IVγ (**42**), for example, X-ray crystallographic analysis showed dihedral angles ϕ_1=13.9, ϕ_2=11.9, ϕ_3=6.6 degrees. These small, positive angles are indicative of an helical arrangement, where the oxygens at C(1) and C(19) distance (the helical pitch) is 3.25 Å.[31] Two intermolecular hydrogen bonds in **40** and **42** pack two symmetry-equivalent molecules into a bis-helical, S-shaped dimer.

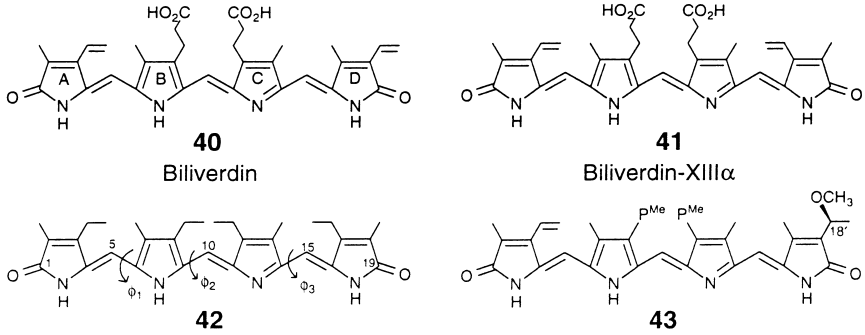

In the absence of an external chiral perturbation (as in biliproteins) the 1,19-dioxobilin (biliverdin) chromophore adopts one of two isoenergetic enantiomeric *M*- or *P*-helical conformations (Scheme 10). Since the conformations will be equally populated, no optical activity is expected from verdin systems such as **40**–**42**. The helical conformers of Scheme 10 are in dynamic equilibrium, and the kinetic parameters of this interconversion process were first estimated in 1979 by dynamic ^{1}H-NMR spectroscopy.[32] For unsymmetrically substituted verdins, e.g., **40**, the symmetry of each conformer in Scheme 10 is C_1. If the verdin is symmetrically substituted, it is C_2, e.g., **41** or **42**. If the helical interconversion is rapid on the nuclear magnetic resonance (NMR) time scale, the former leads phenomenologically to C_s symmetry, and the latter to C_{2v} symmetry. NMR spectroscopy cannot differentiate between C_1 and C_s, or between C_2 and C_{2v} symmetry; thus, the above mentioned biliverdins **40** and **41** are not suitable for study by dynamic NMR in achiral solvents. In order to estimate the kinetic parameters of bilatriene helix inversion, Lehner, Riemer and Schaffner[32] introduced a single stereogenic center, at C(18′) in **43**. In **43** the helical inversion equilibrium is between two diastereomeric pairs of enantiomers [*M*,*S*+*M*,*R*]⇆[*P*,*S*+*P*,*R*], and the equipopulated diastereomeric pairs lacking any symmetry could be detected by low temperature ^{1}H-NMR when the helix inversion was sufficiently slow. In fact, three years earlier a similar sort of diastereomerization adjunct was applied to a study of bilirubin conformational inversion,[33] vide infra. For **43**, the calculated helical interconversion barrier was 42 kJ mol^{-1}, or ~10 kcal mol^{-1} from coalescence temperatures T_c (195–205 K).[32]

Low level theoretical calculations of the optical and chiroptical properties of biliverdin and bilirubin were reported by Wagnière and Blauer in 1975–1976 in connection with studies of induced optical activity from pigment–human serum albumin (HSA) complexes,[34,35] but the first study of a biliverdin chromophore exhibiting natural optical activity was described by Falk and Thirring in 1981.[36] They

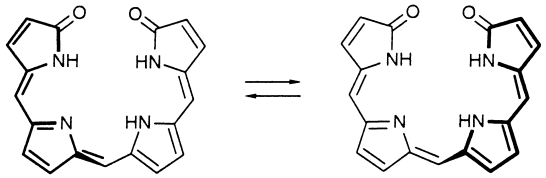

Scheme 10.

synthesized the macrocyclic N(21)–N(24) methano-bridged etiobiliverdin-IVɣ (**44**) in optically active form, employing a partial kinetic resolution with (+)-10-camphor-thiol. The slower reacting enantiomer with estimated 2.1±0.4% ee showed $\Delta\varepsilon_{695}^{max}$ −2.1, $\Delta\varepsilon_{380}^{max}$ +0.56, from which may be predicted that optically pure **44** would exhibit $\Delta\varepsilon_{695}^{max}$ ~ −100±20 (rotatory strength R~ 4.0×10^{-38} cgs), $\Delta\varepsilon_{380}^{max}$ ~ +30±6 (R~ $+1.3\times10^{-38}$ cgs) characteristic of an inherently dissymmetric chromophore.[6,14–16,36,37] A tentative absolute configuration assignment of *M*-helicity was based on a CD sign rule for C_2 symmetric chromophores.[38] From a racemization study, followed by CD, the inversion barrier between the *M*- and *P*-helices of **44** was estimated at $G^{\ddagger}$=105 kJ mol^{-1} at 333 K (~25 kcal mol^{-1})[36] which is considerably higher than that found in unbridged verdin **43**.[32]

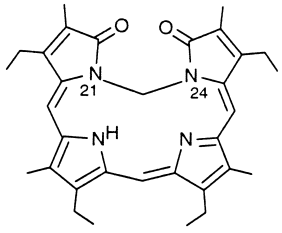

44

A wide variety of optically active biliverdin-IXα or biliverdin-XIIIα amide derivatives were prepared from (*S*)-amino acids, dipeptides and tripeptides and studied by UV–vis and CD spectroscopy by Lehner and Krois.[39–45] The relevant data are presented in Tables 1 and 2. Interestingly, the remote chiral centers of covalently bound (*S*)-amino acids and peptides induced diastereodiscrimination in favor of the *P* (over *M*) biliverdin helix, as evidenced by the strong CD CEs observed as positive visible (660 nm) and negative UV (380 nm) bands. The CE magnitude depended on solvent polarity and the steric demands of the amino acid. With a larger α-substituent steric size (as in **49**, **52** and **53** vs **45** and **47**) stronger CEs were seen. The proposed mechanism for chiral discrimination involves specific intramolecular interactions (mostly hydrogen bonding) between the bilatriene helical backbone (acting as both hydrogen donor and acceptor) and its own two-side chain α-amino acid residues, where the amide NHs act as hydrogen-bond donors and the α-ester carbonyls act as acceptors.[39] When one of these structural elements is absent as in the verdin diester with ethyl (*S*)-lactate (**54** vs **45**) or the bis-amide with (*R*)-amphetamine (**55** vs **47**), the CE magnitude is significantly decreased. The observed nearly additive effect on the CE of bisamide **75** vs mono-amide **76** implied a C_2-symmetrical conformation in which the proximal side chains did not appreciably interact with each other and were situated above and below the bilatriene helix like chiral 'clamps'.[39] However, if additional polar groups were present, then intramolecular interchain interactions were thought to be responsible for decreased Δε values of e.g., the bis-serine and bis-aspartic acid derivatives.[40] If the amino acid C-terminus was derivatized with a bulky alcohol (*tert*-butyl), the CD intensity was markedly decreased as compared to the corresponding methyl esters, e.g., **46** vs **45**, **48** vs **47**, and **50** vs **49**.[40] Obviously, the reason for this attenuation of chiral discrimination is steric: the *tert*-butyl group prevents effective ester side chain carbonyl–bilatriene hydrogen bonding.

Thus, the steric influence of an alkyl group bound to the ester oxygen of the amino acid was opposite to that bound to the chiral center. If the N-terminus was methylated, the CD was also weaker (**51** vs **49**), which shows ineffective discrimination and thus, the importance of amide NH accessible for hydrogen bonding. Not surprisingly, CD from prolyl derivatives **56** and **57** was very weak. In the prolylglycine methyl ester derivative (**58**), effective chiral discrimination returns with the proline–glycine peptide bond NH providing a hydrogen donor and the glycine (although achiral) ester carbonyl — an acceptor.[40] The diastereomeric bis(dipeptide) derivatives **60** and **61** showed identical CD signs of CE with similar magnitudes, although the C-terminal alanine residues were of antipodal configuration. From this it followed that the N-terminal amino acid configuration governed the preferred *P*-helicity of the biliverdin skeleton. An achiral glycine residue at C-terminus (**59**) did not decrease the $\Delta\varepsilon$ value, but when at N-terminus (**64**, **65**) diastereoselection was lost. The most prominent feature of bis(tripeptides) of **40** was the significant increase of optical activity compared with bis(dipeptides), **66** vs **60**, **69** vs **63**.[41] Less sterically crowded alanine (in **66**) was more effective than valine in **68**. One unit of glycine at all permutation positions (**69**–**71**) did not affect the selectivity. Discussing the mechanism of the observed diastereoselection, it was pointed out that in di- and tripeptide chains with multiple H-bonds donor–acceptor sites, interchain interactions became apparent, as evidenced by higher discrimination in mono-derivative **78** (Table 2) as compared to bis-derivatives **62** and **77**.[41]

From the systematic variations of peptide chains in Tables 1 and 2 it was shown that lengthening the peptide beyond a tripeptide did not increase the helical excess, cf., **60** vs **66** and **67**. The hetero tri- and tetrapeptides **72**–**74** exhibited invariant maximum $\Delta\varepsilon$ values, and this was thus considered as further evidence for complete chiral discrimination of biliverdin undisturbed helices, as in **66** and **67**. Compiling these results, Krois and Lehner concluded that a homochiral biliverdin helix should have $|\Delta\varepsilon|_{660}$ ~100–110 and $|\Delta\varepsilon|_{380}$ ~140–150 corresponding to rotatory strengths R ~4.0×10^{-38} and 4.6×10^{-38} cgs, respectively.[42] The longer wavelength $\Delta\varepsilon$ value coincided well with that estimated for **44** but the near UV $\Delta\varepsilon$ value did not.[36] This discrepancy might be explained with more closed helix of **44** (helical pitch ~2.0 Å) while the derivatives in Tables 1 and 2 were all with a virtually undisturbed helix (pitch ~3.3 Å), as judged by UV–vis spectral similarities with biliverdin-IXα (**40**) and XIIIα (**41**) dimethyl esters.

In general, all compounds listed in Tables 1 and 2 showed a decreasing CD with increasing solvent dipole moment rather than solvent dielectric constant. In ethanol, $\Delta\varepsilon$ values were the lowest, which suggested intermolecular competition of the solvent for hydrogen-bonding sites, and thus disruption of the network of intramolecular hydrogen bonds dictating a *P*-helicity chromophore.

Titration of **45**, **49**, **52**, **54**, **55** and **65** with TFA in benzene, chloroform, or ethanol caused drastic changes in their CD spectra: the longer wavelength CE of **45** split [$\Delta\varepsilon_{733}^{max}$ −48, $\Delta\varepsilon_{657}^{max}$ +48 (C_6H_6+TFA)] and that of **55** split and intensified [$\Delta\varepsilon_{735}^{max}$ −140, $\Delta\varepsilon_{657}^{max}$ +125 (C_6H_6+TFA)] at optimum conditions. Equilibria between monomeric monoprotonated, aggregated monoprotonated, diprotonated, etc., species depending on solvent hydrogen-bonding ability, concentration of both solute and acid, and their ratio were proposed to explain the spectral changes.[43]

CD spectral-based assignments of biliverdin chromophore helicity in model compounds such as **44**–**78** were initially made from theoretical calculations[34,35] and an empirical CD rule.[38] The first firm correlation between CE sign and biliverdin helicity came in 1987 from an X-ray crystallographic analysis of the bilin binding protein of the butterfly *Pieris brassicae* at 2.0 Å resolution.[46] It clearly showed that the biliverdin-IXγ (**79**, pterobilin) chromophore had adopted a right-handed (*P*) helicity with a (4*Z*,9*Z*,15*Z*) configuration, all-synperiplanar conformation, and a helical pitch of 5.5 Å. Though achiral by structure, the chromophore of **79** displayed strong optical activity in the native protein-bound state: $\Delta\varepsilon\sim$ +90 for the visible band near 650 nm and $\Delta\varepsilon\sim$ −190 for the UV band near 380 nm (Fig. 8),[46] but became inactive

Table 1
Circular dichroism data for optically active bis-amides and esters of biliverdin-IXα with (*S*)-amino acids and peptides

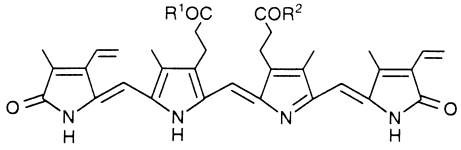

	$R^1 = R^2 =$	$\Delta\varepsilon^{max}$ (λ^{max}) in Benzene			$R^1 = R^2 =$	$\Delta\varepsilon^{max}$ (λ^{max}) in $CHCl_3$	
45	Ala-O*Me*	+39.0 (657)	−56.9 (378)		Ala-NH*Me*	+44.5 (665)	−61.9 (374)
46	Ala-O*tBu*	+12.2 (652)	−19.8 (379)	**59**	Ala-Gly-O*Me*	+56.4 (657)	−90.7 (375)
47	Phe-O*Me*	+39.9 (662)	−64.3 (378)	**60**	Ala-Ala-O*Me*	+28.4 (655)	−43.9 (378)
48	Phe-O*tBu*	+26.2 (661)	−45.7 (380)	**61**	Ala-(*R*)-Ala-O*Me*	+22.1 (658)	−36.6 (377)
49	Val-O*Me*	+52.9 (660)	−77.9 (378)		Ala-Val-O*Me*	+16.2 (648)	−27.6 (377)
50	Val-O*tBu*	+19.8 (658)	−33.1 (380)	**62**	Val-NH*Me*	+41.3 (659)	−61.3 (376)
51	Val(Me)-O*Me*	+23.3 (660)	−35.3 (380)	**63**	Val-Gly-O*Me*	+38.8 (659)	−62.8 (377)
	Met-O*Me*	+42.0 (660)	−63.9 (378)		Val-Ala-O*Me*	+20.2 (650)	−33.0 (378)
52	Leu-O*Me*	+49.1 (660)	−75.1 (378)		Val-Val-O*Me*	+9.6 (650)	−16.3 (377)
53	Trp-O*Me*	+50.2 (664)	−81.7 (381)		Val-(*R*)-Val-O*Me*	+7.2 (645)	−12.7 (377)
54	(*S*)-OCH(CH_3)$CO_2C_2H_5$	+1.2 (660)	−1.4 (365)	**64**	Gly-Ala-O*Me*	0.0	−0.8 (375)
55	(*R*)-NHCH(CH_3)$CH_2C_6H_5$	+10.0 (666)	−17.7 (383)	**65**	Gly-Val-O*Me*	+2.2 (655)	−3.9 (378)
56	Pro-O*Me*	+3.1 (667)	−5.5 (377)	**66**	Ala-Ala-Ala-O*Me*	+109.0 (655)	−151.0 (375)
57	Pro-O*Bzl*	+3.8 (663)	−6.0 (377)	**67**	Ala-Ala-Ala-Ala-O*Me*	+100.0 (650)	−142.4 (378)
	Ser-O*Me*	+28.8 (664)	−49.6 (378)	**68**	Val-Val-Val-O*Me*	+72.0 (640)	−111.0 (378)
	Asp(O*Me*)-O*Me*	+29.9 (664)	−49.1 (379)	**69**	Val-Val-Gly-O*Me*	+73.9 (640)	−112.2 (375)
58	Pro-Gly-O*Me*	+52.0 (661)	−78.9 (379)	**70**	Val-Gly-Val-O*Me*	+97.3 (658)	−129.1 (378)
	Pro-Gly-O*tBu*	+3.0 (663)	−4.7 (400)	**71**	Gly-Val-Val-O*Me*	+80.2 (644)	−119.4 (376)
	Pro-Leu-O*Me*	+3.3 (658)	−6.9 (382)		Gly-Gly-Val-O*Me*	+3.9 (650)	−4.1 (375)
	Leu-Leu-O*Me*	+13.2 (650)	−20.4 (375)		Ala-Ala-NH*Me*	+95.0 (655)	−140.4 (376)
72	Leu-Gly-Pro-O*Me*	+102.9 (662)	−147.0 (381)		Ala-Ala-Gly-O*Me*	+98.9 (655)	−141.5 (377)
73	Val-Pro-Ala-Val-O*Me*	+101.6 (660)	−140.0 (380)		Ala-Ala-Pro-Ala-Ala-O*Me*	+63.7(650)	−102.1(379)
74	Ala-Pro-Ala-Val-O*Me*	+101.3 (655)	−140.0 (380)				
	Val-Val-Pro-O*Me*	+45.2 (635)	−72.3 (375)				
	Ala-Pro-Ala-Ala-O*Me*	+100.6 (658)	−141.5 (380)				
	Val-Val-Pro-Ala-Ala-O*Me*	+32.8 (635)	−46.6 (376)				
	Ala-Val-Pro-Ala-Val-O*Me*	+49.8 (642)	−71.3 (383)				

R^1 = arbitrary assignment	$R^2 =$	$\Delta\varepsilon^{max}$ (λ^{max}) in Benzene	
Ala-O*tBu*	O*Me*	+6.4 (656)	−10.5 (377)
O*Me*	Ala-O*tBu*	+6.9 (654)	−10.9 (377)
Asp(O*Me*)-O*Me*	O*Me*	+19.2 (663)	−28.9 (377)
O*Me*	Asp(O*Me*)-O*Me*	+22.0 (665)	−34.6 (379)
Val(*Me*)-O*Me*	O*Me*	+8.7 (662)	−12.4 (380)
O*Me*	Val(*Me*)-O*Me*	+8.0 (662)	−10.7 (380)
Ala-Val-Pro-Ala-Val-O*Me*	O*Me*	+24.2 (655)	−36.7 (376)

after urea denaturation of the protein.[47] The intense Cotton effects were induced by enantioselective embedding through non-covalent binding to the protein by only a few hydrogen bonds (the nitrogen atoms of **79** were tightly associated with two water molecules and the carboxylic acids groups were exposed to solvent) and numerous Van der Waals interactions that oriented the two bilatriene faces in environments of very different polarity.

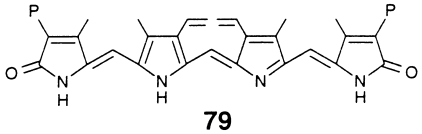

79

More recently, the crystal structure determination of an apomyoglobin–biliverdin **40** complex at 1.4

Table 2
Circular dichroism data for optically active bis-amides and esters of biliverdin-XIIIα with (*S*)-amino acids and peptides

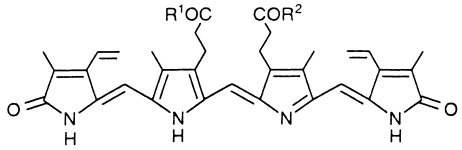

	$\Delta\varepsilon^{max}$ (λ^{max}) in Benzene			$\Delta\varepsilon^{max}$ (λ^{max}) in $CHCl_3$	
75 R^1=R^2= Ala-O*Me*	+36.6 (649)	−45.5 (372)	**77** R^1=R^2= Val-NH*Me*	+36.9 (650)	−48.9 (373)
76 R^1=Ala-O*Me*, R^2=O*Me*	+21.0 (650)	−24.6 (372)	**78** R^1=Val-NH*Me*, R^2=O*Me*	+63.5 (659)	−82.9 (373)
			R^1=R^2= Ala-Gly-O*Me*	+55.4 (652)	−77.9 (372)
			R^1=Ala-Gly-O*Me*, R^2=O*Me*	+55.0(657)	−68.2 (373)
			R^1=R^2= Val-Val-O*Me*	+10.8 (644)	−15.9 (380)
			R^1=Val-Val-O*Me*, R^2=O*Me*	+9.5 (650)	−13.9 (373)
			R^1=R^2=Val-Gly-Val-O*Me*	+79.5 (652)	− 89.8 (375)
			R^1=Val-Gly-Val-O*Me*, R^2=O*Me*	+96.6(658)	−106.1(377)

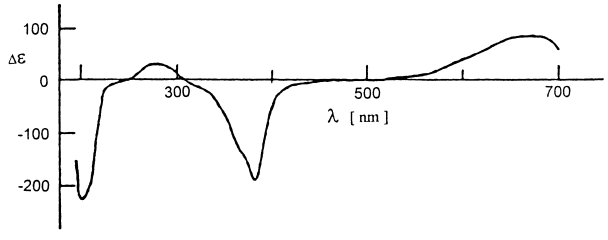

Figure 8. Circular dichroism spectrum of biliverdin-IXγ (**79**) bound to the bilin binding protein of the butterfly *Pieris brassicae*. Redrawn from Huber et al.[46]

Å resolution[48] confirmed the correlation that a *P*-helical embedded chromophore **40** is associated with a positive CD band in the visible and negative UV band [ICD +43 (700), −63 (380) in H_2O].[49]

A separate group of bis(tripeptides) of **40** and **41** (Table 3) with proline at the N-terminus exhibited a remarkable tendency to adopt stretched conformations — as concluded from the ratio UV/vis dipole strengths $f=D_{UV}/D_{VIS}$. The reference here is f=2.41 for dimethyl ester of **40**. For **80**–**84**, f=1.3–1.7, and a strong solvatochromic effect was found, as well as sensitivity to the steric requirements of the second amino acid residue. The CD data of **80**–**84** were more difficult to comprehend, since neither the Δε value of any homochiral stretched species nor the fractional population and extent of chiral discrimination were known. Comparison of mono- with bis-peptide derivatives **85**–**90** suggested that the susceptibility of UV–vis spectra toward the bulkiness of the second amino acid residue was mostly due to intramolecular interchain interactions. Interestingly, for the monopeptide **86**, with intermediate f value, the CD complex spectrum appeared as superposition of spectra corresponding to two distinct species with opposite rotatory strengths. One of the species was thought to adopt a stretched conformation. Since helical biliverdin peptides composed of (*S*)-α-amino acids showed a preference for the *P*-helicity (Tables 1 and 2), the CD sign reversal observed only in **88** and **90** (Table 3) was attributed also to a (*Z*, *Z*, *Z*, *anti*, *syn*, *syn*) stretched chromophore. A model for binding of this and of the coiled all-*syn* chromophore to the sequence Pro–X–Y was proposed.[44,45]

Table 3
Circular dichroism data for optically active bis-amides of biliverdin-IXα, XIIIα and a cyclic analog with (*S*)-amino acid peptides

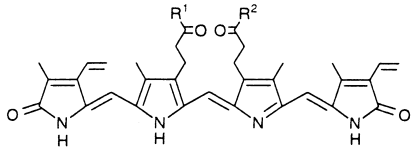

	$R^1 = R^2 =$ in Benzene	f	$\Delta\varepsilon^{max}$ (λ^{max})	$\Delta\varepsilon^{max}$ (λ^{max})
	Pro-Ala-Ala-O*Me*	2.42	+ 102.0 (650)	- 121.9 (380)
	Pro-Ala-Val-O*Me*	2.37	+ 98.0 (656)	- 110.0 (382)
80	Pro-Leu-Gly-O*Et*	1.68	+ 34.9 (662)	- 49.5 (382)
81	Pro-Leu-Leu-O*Me*	1.70	+ 59.4 (660)	- 82.7 (378)
82	Pro-Leu-Val-O*Me*	1.60	+ 41.6 (659)	- 51.9 (381)
83	Pro-Val-Val-O*Me*	1.47	+ 49.6 (653)	- 66.0 (385)
84	Pro-Val-(*R*)-Val-O*Me*	1.37	+ 61.3 (655)	- 84.1 (384)
	Leu-Pro-Leu-Leu-O*Me*	2.75	+ 105.6 (657)	- 144.1 (377)

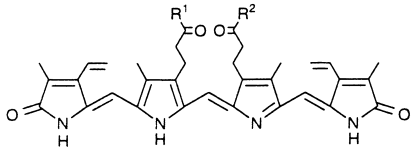

	arbitrary assignment			
85	R^1=R^2= Pro-Ala-Ala-O*Me*	2.03	+ 94.6 (652)	- 99.6 (378)
86	R^1= Pro-Ala-Ala-O*Me*, R^2=O*Me*	1.57	+ 11.5 (670)	- 2.4 (407)
87	R^1=R^2= Pro-Leu-Val-O*Me*	1.41	+ 44.0 (656)	- 56.3 (381)
88	R^1= Pro-Leu-Val-O*Me*, R^2=O*Me*	1.29	- 37.2 (645)	+ 49.5 (385)
89	R^1=R^2= Pro-Val-(*R*)-Val-O*Me*	1.20	+ 52.0 (645)	- 61.0 (381)
90	R^1= Pro-Val-(*R*)-Val-O*Me*, R^2=O*Me*	1.31	- 29.9 (645)	+ 42.0 (384)
	R^1=R^2= Ala-Pro-Ala-Ala-O*Me*	2.22	+ 94.6 (651)	- 115.7 (374)
	R^1=Ala-Pro-Ala-Ala-O*Me*, R^2=O*Me*	2.17	+ 95.1 (655)	- 114.1 (373)
	R^1=R^2= Leu-Gly-Pro-O*Me*	2.11	+ 96.1 (655)	- 115.6 (376)
	R^1= Leu-Gly-Pro-O*Me*, R^2= O*Me*	2.16	+ 101.1 (658)	- 120.1 (377)

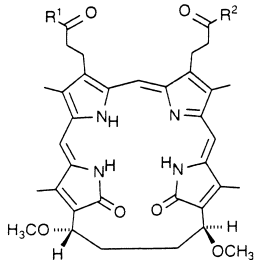

R^1=R^2= Pro-Val-(*R*)-Val-O*Me*	2.44	+ 74.5 (648)	- 93.7 (379)
R^1= Pro-Val-(*R*)-Val-O*Me*, R^2=O*Me*	2.33	+ 43.3 (648)	- 51.9 (379)

5. Cyclic biliverdins

When treated with acidic methanol, biliverdin-IIIα dimethyl ester underwent ring closure between both *exo*-vinyl groups with consecutive addition of two methoxy groups and oxidation leading to a mixture of **91**+**92**. This reaction was not observed for the dimethyl esters of **40** or **41**, which do not

have two *exo*-vinyl groups, but took place in biliverdin-IIIα due to the close proximity of its 2,18-vinyl groups, as found in a helical biliverdin conformation.[50] TLC at 258 K afforded separation of two thermally interconverting pairs of enantiomers (**91A**+**B**) and (**92A**+**B**). ^{1}H-NMR revealed C_2-symmetrical structures, and NOE experiments allowed for the assignment of the relative configuration.[50] A third possible *meso* diastereomer **93** was formed only in minute amounts. Since racemic **91A**+**B** and racemic **92A**+**B** had the same C(1′) and C(4′) configuration, configurational change of the third chirality element — the handedness of helically shaped bilatriene backbone, should result in mutual conversion of diastereomers (Eqs. 1 and 2) but helix inversion in the *meso* isomer **93** should afford the corresponding antipode (Eq. 3).

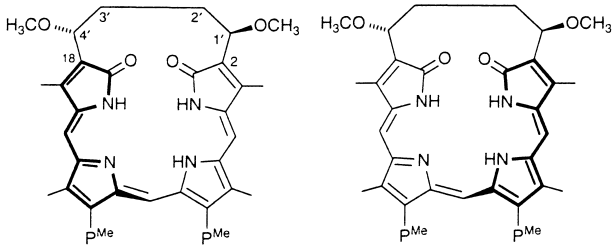

91A (*M*,1′*R*,4′*R*)	−127.3 (652)[a] +214.8 (370)	**91B** (*P*,1′*S*,4′*S*)	+125.8 (652)[b] −212.4 (370)
92B (*M*,1′*S*,4′*S*)	−140.8 (653)[a] +214.2 (385)	**92A** (*P*,1′*R*,4′*R*)	+137.5 (653)[b] −207.9 (385)

[a,b] in C_2H_5OH; interchangeable Δε values since the chiral centers configuration is not known.

(*M*,1′*R*,4′*R*)-**91A** ⇌ (*P*,1′*R*,4′*R*)-**92A** (1)

σ

(*P*,1′*S*,4′*S*)-**91B** ⇌ (*M*,1′*S*,4′*S*)-**92B** (2)

(*P*,1′*R*,4′*S*)-**93** ⇌ (*M*,1′*R*,4′*S*)-**93** (3)

σ

CD spectroscopy was used to monitor the racemization rate of *M*-helically enriched (**91A**+**92B**) over temperature range 277–312 K. An interconversion barrier of $\Delta G^{\ddagger}$=85–90 kJ mol^{-1} at 293 K, an equilibration half-life of 230 s, and $\Delta H^{\ddagger}$=77.7 kJ mol^{-1}, $\Delta S^{\ddagger}$=38 J mol^{-1} K^{-1} were estimated.[51] For the monocation, $\Delta G^{\ddagger}$=80–84 kJ mol^{-1} was determined.[52] The results were confirmed for the monohydroxy derivatives and for **93**. This interconversion barrier is almost twice as high as that reported for nonbridged biliverdin **43**, which is presumably a consequence of the restrictions imposed by the ‘unnatural’ four carbon belt.

Optical resolution and separation of a four component mixture **91**+**92** were accomplished by a first order asymmetric transformation. In presence of (−)-(*R*)-mandelic acid the equilibria expression Eqs. 1 and 2 were shifted toward *M*-helical isomers of **91A** and **92B** according to the small energy difference between diastereomers **91A**+**B** and **92A**+**B**, which was of the order of chiral intermolecular discriminating interactions. The discriminatory efficiency was strongest in the nonpolar solvent benzene. Four cycles of room temperature equilibration starting from a total mixture **91**+**92** and (−)-(*R*)-mandelic acid was followed by TLC separation at 258 K to afford optically pure **91A** and **92B**. The corresponding enantiomeric helical entities were obtained from **91A** and **92B** after room temperature equilibration in CH_2Cl_2 for **92A** (Eq. 1) and in CCl_4 for **91B** (Eq. 2), respectively. The CD data of **91** and **92** were characteristic of completely resolved *M*- and *P*-helical chromophores, as compared, for instance to bis(tetrapeptide) **73**. However, the UV CD band was found to be more influenced by substitution pattern. Hence, the rotatory strength of the visible CD band was considered to be more a general property of a helical bilatriene chromophore.[53]

A protonation equilibrium during the optical resolution with mandelic acid could not be discerned since the basicity of constrained biliverdins **91** and **92** was later found to be at least three orders of magnitude lower than that of open chain **40** dimethyl ester, which is known to adopt a stretched conformation in the monoprotonated form. Titration with H_2SO_4 of a sample enriched in **92A** in CH_3OH drastically changed the λ^{max} of the visible CD band, from $\Delta\varepsilon^{max}_{652}$ +90.2 (neutral **92A**) to $\Delta\varepsilon^{max}_{719}$ +87.0 (monoprotonated **92A**) while the UV CD band was almost unaffected.[54] The invariability of the CD sign meant that the predictions for vis and UV CD signs deduced for the *P*- and *M*-helix of neutral bilatrienes[35] are equally applicable to the corresponding protonated helical chromophores.

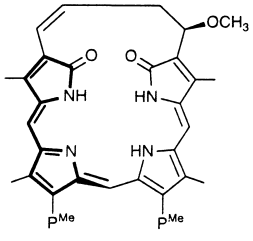

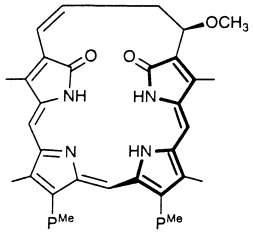

94A (***M***,1′*R*)	−122.9 (652)[a] +241.7 (378)	**94B** (***P***,1′*S*)	+125.4 (652)[b] −245.3 (378)
95B (***M***,1′*S*)	−125.5 (652)[a] +243.4 (377)	**95A** (***P***,1′*R*)	+126.6 (652)[b] −242.3 (375)

[a,b] in CH_3OH; interchangeable Δε values since the chiral center configuration is not known.

A similar resolution–separation technique using (−)-(*R*)-cyclohexylhydroxyacetic acid afforded verdins **94** and **95**.[55] The interconversion $M \leftrightharpoons P$ barrier for neutral **94**/**95** determined by CD was $\Delta G^{\ddagger}$=99–102 kJ mol^{-1}, and $\Delta G^{\ddagger}$=96–98 kJ mol^{-1} — for their monocations both at 293 K. This 10–15 kJ mol^{-1} increase in the barrier above that for **91** and **92** indicates the additional kinetic stability in **94** and **95** imparted by the double bond in the belt.[52]

Table 4
Circluar dichroism data for cyclic esters of chiral mesobiliverdin-XIIIα in chloroform

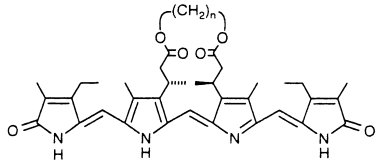

	Ester	$\Delta\varepsilon^{max}$ (λ^{max})	$\Delta\varepsilon^{max}$ (λ^{max})
96	dimethyl ester	+ 6.1 (644)	- 14.3 (365)
97	n=l	+ 8.0 (637)	- 23.6 (362)
98	n=2	- 9.2 (630)	+25.5 (363)
99	n=3	- 11.1 (642)	+34.5 (363)
100	n=4	- 3.3 (649)	+ 6.6 (371)
101	n=5	+11.8 (641)	- 31.7 (364)
102	n=6	+ 7.7 (629)	- 20.4 (364)

Introduction of two chiral centers in immediate proximity to the biliverdin core as in (β*S*,β′*S*)-dimethylmesobiliverdin-XIIIα dimethyl ester (**96**) and its cyclic ester congeners **97**–**102** was not accompanied with appreciable helix diastereoselection. Their CD data (Table 4) indicate that while the noncyclic ester **96** as well as the longest belted (**101**, **102**) and the shortest belted (**97**) cyclic esters slightly preferred a *P*-helicity, in medium length cyclic esters (**98**, **99** and **100**), the *M*-helicity dominated.[56] The reason for the differing choice of helicity is not obvious, but the helical preference is not strong because the CD CE magnitudes are only 5–10% of the maximum Δε values reported.

6. Biliproteins: phycoerythrin, phycocyanin, phytochrome and their synthetic analogs

The most exhaustively studied group of linear tetrapyrroles containing the structural dipyrrin unit **I** is that of biliprotein[57] chromophores and their synthetic models. Common among them is (i) a conjugated 2,3-dihydropyrrolinone ring (A), which is covalently bound to the apoprotein, and (ii) a conjugated (**104**, **105**) or unconjugated (**103**) D-ring. A detailed review on the stereochemistry of biliprotein chromophores was provided by Gossauer in 1983.[58] The applications of chiroptical spectroscopy in studies related to stereochemical problems in biliproteins have generally focussed on three areas: (i) native systems: phycocyanins, phycoerythrins, phytochrome (Fig. 1) — where the nonbonded interactions between apoprotein and chromophores are as intact as possible; (ii) denaturated or partially proteolitically digested systems, where the lysine–chromophore covalent bond is still present; and (iii) natural or synthetic model systems lacking this bond, where the information on the C(3) and C(3^1) stereogenic centers is lost, but the chromophore stereochemistry alone is conveniently accessible. The last area is the most comprehensive, and we shall begin our discussions with it.

Early ORD studies of the urobilin (**2**) (Section 2) obtained from **103** by catalytic hydrogenation, followed by reoxidation (by I_2) to restore the dipyrrin system showed that the phycoerythrobilin (**103**) absolute configuration at C(16) is the same (*R*) as that of (+)-**2**.[59] In 1973, H. Brockmann, Jr. and G. Knobloch applied ORD to the (−)-2-methyl-(3*E*)-ethylidenesuccinimide isolated after chromic acid oxidation of **104** dimethyl ester thereby chemically correlating the former enantiomer with (+)-(2*R*, 3*R*)-**11** (see Section 3). From this study, the absolute configuration of phycocyanobilin was shown to be (2*R*).[60] The same (2*R*) configuration was later inferred for phycoerythrins.[61]

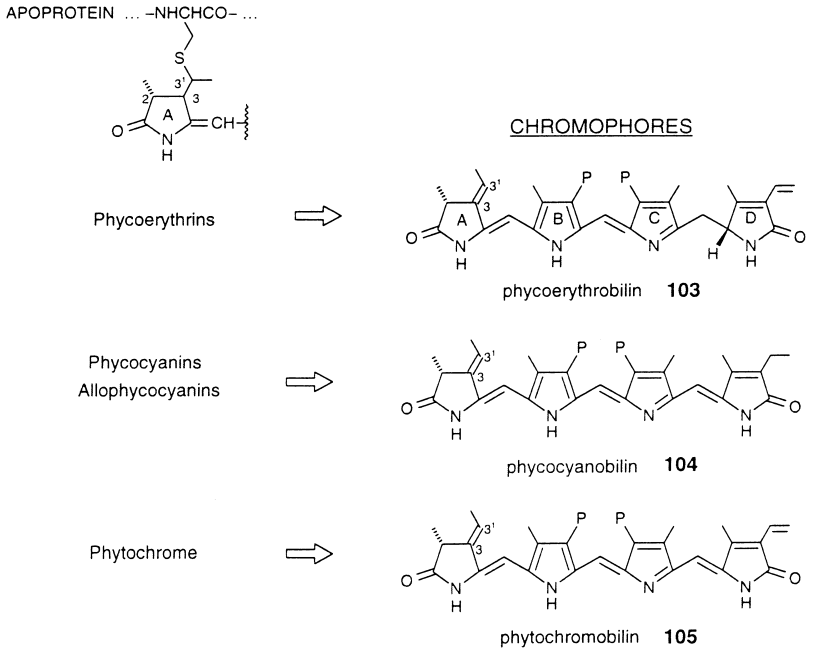

An unequivocal proof of the absolute configuration of phycoerythrobilin dimethyl ester came in its total synthesis, as reported by Gossauer and Weller in 1978.[62] They used an independent route to urobilin **24** in order to correlate the absolute configuration of previously known acid (+)-(*R*)-**13** with that of the new optically active aldehyde (+)-(*R*)-**23** methyl ester (**112**). The last was obtained from (+)-(*R*)-**111** (Scheme 11) in which the α-methylfenchyl residue served as a readily removable (by TFA) chiral auxiliary used in the separation of the diastereomeric selenides **110A** and **110B** by simple recrystallization.

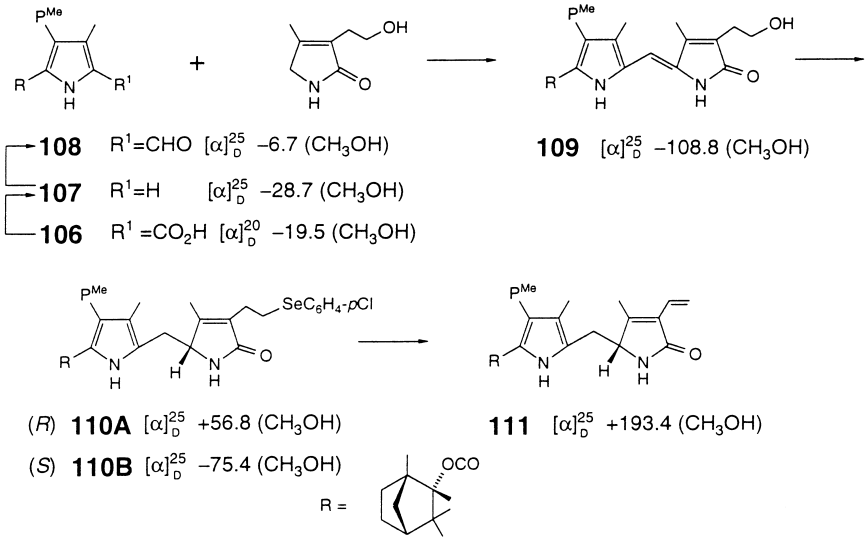

Scheme 11.

Then the aldehyde **112** was condensed with racemic **113** to afford phycoerythrobilin dimethyl ester (**103 DME**) and its C(2) epimer **103A DME** which were separated (Scheme 12). The analytical data, including comparisons of ORD and CD spectra, however, did not differentiate between synthetic **103**

DME and **103A DME**, and **103 DME** obtained from natural sources, thus indicating a minimal influence of the C(2) configuration on the chiroptical properties of these chromophores (Fig. 9). Chromic acid degradation of synthetic **103 DME** gave the same (−)-(2*R*)-methyl-(3*E*)-ethylidenesuccinimide as that obtained from the natural pigment. Thus, both the synthetic **103 DME** and the natural phycoerythrobilin (**103**) possessed the (2*R*,16*R*) absolute configuration.[62] The ORD data of precursors **106**–**112** and products **103 DME**, **103A DME** were also made available in this study.

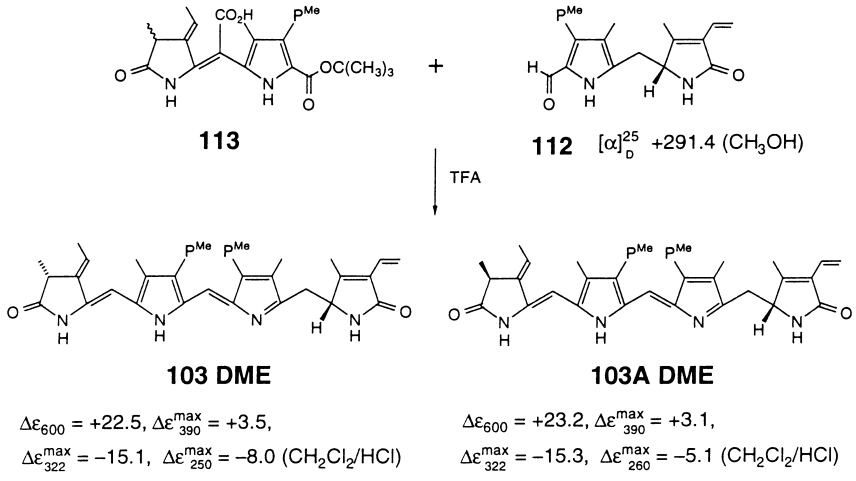

Scheme 12.

Shortly thereafter, Rapoport et al. reported on a comparative study, using 360 MHz ^{1}H-NMR, of a heptapeptide-linked phycocyanobilin (**114**) obtained from mild BrCN cleavage of C-phycocyanin and its synthetic peptide moiety.[63] From earlier work[60,61,64] and the *trans*-geometry at C(2) and C(3) of ring A, which was assumed but later proven,[65] the (2*R*,3*R*,3^1*R*) absolute configuration was assigned to **114**. Its CD spectra in D_2O appeared distinctively different at 5.7×10^{-5} M and 2.2×10^{-3} M concentrations, with negative and positive long wavelength CEs, respectively, near 675 nm. The data suggest prosthetic group dimerization, perhaps through π-complex formation. Such concentration dependence was not found for Cys-Tyr-Arg tripeptide from B-phycoerythrin.[66] The same (2*R**,3*R**,3^1*R**) relative configuration as in **114** is found in phytochrome[65,67] and probably in phycoerythrin.[66] Although the same absolute configuration at C(2) is found in **103** and **104** (that of **105** has not been explicitly reported), caution was raised[63,65] that the stereochemical identity of all three phycocyanobilin groups in C-phycocyanin had not been firmly established.

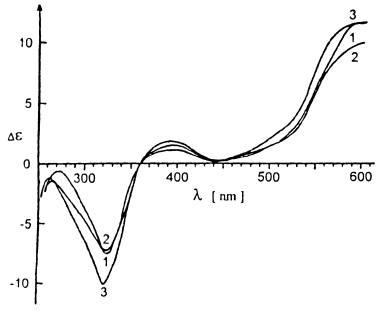

Figure 9. Circular dichroism spectra of CH_2Cl_2 solutions of synthetic (2*R*,16*R*)-**103 DME** (Spectrum 1), (2*S*,16*R*)-**103A DME** (Spectrum 2), and dimethyl ester of natural (2*R*,16*R*)-phycoerythrobilin (**103**) from C-phycoerythrin (Spectrum 3). Redrawn from Gossauer and Weller[62]

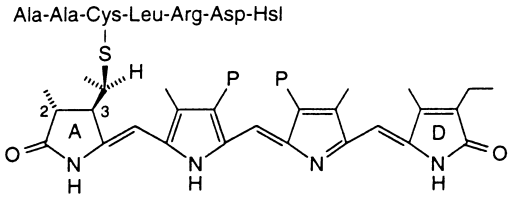

114 Phycocyanobilin Derivative

$\Delta\varepsilon$ ~ –9 (693), $\Delta\varepsilon$ ~ –2 (400), $\Delta\varepsilon$ ~ +7 (340)

Hsl = homoserine lactone

In the mid-1980s, 2,3-dihydrobilatriene-*abc* structures represented by **115** (Table 5) and its derivatives were examined extensively as phytochrome chromophore models. Methyl ester **115** was resolved by recycling chromatography on triacetylcellulose to constant rotation ($[\alpha]_{436}^{20}$ −5480 (C_2H_5OH)) while its constituent A–B ring 2,3-dihydrodipyrrinone was only partially resolved ($\Delta\varepsilon_{303}^{max}$ +2.1).[68] Their absolute configuration was at the time, however, unknown. The presence of the lone chiral center at C(3) in **115** added only a little stabilization of *P*-helix as concluded from low CD Cotton effects[68] which correlated with the influence of single C(2) chiral center.[62] This is in accord with the low helix interconversion barrier for **115**, estimated to be much less than 20 kJ mol^{-1}.[1] Earlier, Falk, Kapl and Medinger had reported a systematic investigation on the chiroptical properties of 2,3-dihydrobilatriene-*abc* **115** analogs with attached amino acid, dipeptide, or cholesterol residues,[69] (Tables 5 and 6) — this before the data in Tables 1–3 had been accumulated. Neither the steric size of an α-alkyl substituent in the amino acid (**118** vs **117**) nor that of the ester group (**116** vs **117**) influenced the magnitude of $\Delta\varepsilon$ significantly. Hydrophobic interactions between the cholesterol residue and the chromophore backbone in **125** also did not contribute significantly to the helix selection.[70,71] The effect of chiral discrimination was strongly diminished when similar chiral appendices were attached to the C(12) propionic acid, i.e., farther removed from the bilatriene skeleton, see Table 6 vs Table 5. However, the presence of a dipeptide bond (**121**, **122**) was found to increase the helix stereoselection.[69] From the presented data, Falk et al.[69] concluded that intramolecular dipole–dipole interactions between the chromophore backbone and the chiral moiety were responsible for the *M*- or *P*-selection, with hydrogen-bonding being less important. Comparison of the CD data for pigments **123** and **127** with **124** and **128** supports this conclusion, as the permanent dipole moments in the second pair are larger than in the first pair, and, correspondingly, the helical excess is larger. The CD CE magnitudes of **119A**, **122A** and **126** were strongly solvent dependent, reaching a plateau in low dielectric constant solvents. From these limiting values, it was concluded that enantio-pure helical chromophore of this chromophore type should have a $|\Delta\varepsilon|$ maximum for the visible band of ~60 and for the UV band, ~100.[69] Temperature dependent CD measurements of **119A**[69] and **120A**[70] gave $\Delta H°$ ~5 kJ mol^{-1} (and $\Delta H°$ ~2 kJ mol^{-1} in **126**[69]) for the equilibrium between helical enantiomorphs thought to be important in the conformational preponderance in biliproteins.

Extremely intense CD spectra were measured for C(3)/C(3^1) adducts of phycoerythrobilin dimethyl ester (**103 DME**) and phycocyanobilin dimethyl ester (**104 DME**) with cysteine and glutathione (Table 7). These, too, were interpreted in terms of helical chromophore geometry and related to the configuration at C(3^1).[72] See also more recent data from Grubmayr et al.[73–75] in the following structures.

Table 5
Circular dichroism data in $CHCl_3$ solvent for 2,3-dihydrobilatriene-*abc* analogs of phycocyanin and phytochrome

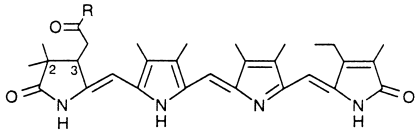

	R[a]	$\Delta\varepsilon^{max}$ (λ^{max})	
115	OCH_3	+ 11.6(594)	- 19.3(345)
116A	Ala-O*tBu*	- 37.2(600)	+ 55.4(350)
116B	Ala-O*tBu*	+ 31.6(605)	- 59.0(350)
117A	Ala-O*Et*	- 47.3(596)	+ 71.6(350)
117B	Ala-O*Et*	+ 45.1(603)	- 76.2(347)
118A	Leu-O*Et*	- 53.1(600)	+ 86.3(350)
118B	Leu-O*Et*	+ 48.4(600)	- 99.2(350)
119A	Trp-O*Et*	+ 54.5(600)	- 97.7(350)
119B	Trp-O*Et*	- 59.9(595)	+ 97.7(350)
120A	Lys(*t-Boc*)-O*tBu*	+ 52.0(582)	- 76.1(348)
120B	Lys(*t-Boc*)-O*tBu*	- 45.0(580)	+ 70.0(347)
	Lys(*tBoc*)-O*tBu*(4*Z*,9*Z*,15*E*)	+9.4(610)	-40.0(348)
121A	Ala-Gly-O*Et*	-57.2(600)	+99.9(350)
121B	Ala-Gly-O*Et*	+ 46.5(600)	- 86.0(350)
122A	Ala-Ala-O*Et*	- 62.6(600)	+ 94.9(350)
122B	Ala-Ala-O*Et*	+49.8(600)	- 81.1(350)
123A	(*R*)-NHCH(CH_3)C_6H_5	- 41.3(600)	+ 68.6(352)
123B	(*R*)-NHCH(CH_3)C_6H_5	+ 38.6(595)	- 72.7(351)
124A	(*R*)-NHCH(CH_3)C_6H_4-*p*-NO_2	+49.9(605)	-102.0(355)
124B	(*R*)-NHCH(CH_3)C_6H_4-*p*-NO_2	-53.3(605)	+ 92.5(355)
125	Cholesteryl (3*R*)-(4*Z*,9*Z*,15*Z*)[b]	-1.9(580)	- 4.8(344)
	Cholesteryl (3*R*)-(4*Z*,9*Z*,15*E*)[b]	-0.3(550) (CCl_4)	

[a] All (*S*)-amino acids; **A** and **B** were epimeric at C(3) and on TLC gave R_f (**A**) > R_f (**B**).
[b] The (3*R*) configuration was deduced from NMR data.[71]

Table 6
Circular dichroism data in $CHCl_3$ solvent for chiral 2,3-dihydrobilatriene-*abc* analogs

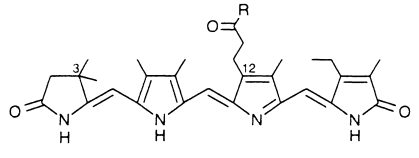

	R	$\Delta\varepsilon^{max}$ (λ^{max})	
126	Ala-O*Et*	+ 17.0 (580)	- 26.0 (344)
	Phe-O*Et*	+ 13.5 (576)	- 24.0 (345)
	Lys(*tBoc*)-O*Et*	+ 12.8 (577)	- 19.0 (344)
	ω-Lys(α-*Z*)-O*Et*	~0.0	
127	(*R*)-NHCH(CH_3) C_6H_5	~0.0	
128	(*R*)-NHCH(CH_3) C_6H_4-*p*-NO_2	+ 3.5 (597)	- 17.0 (348)
	Cholesteryl	- 1.0 (548)	+ 3.0 (354)

Table 7
Circular dichroism data in $CHCl_3$ solvent for phycoerythrobilin dimethyl ester (**103 DME**) and phycocyanobilin dimethyl ester (**104 DME**) and their C(3)/C(3′) adducts

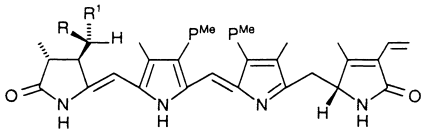

	$\Delta\varepsilon^{max}$ (λ^{max})	
103 DME	+31.4 (526)	−32.4 (310)
R= CH_3, R^1= (*R*)-$SCH_2CH(NH_2)CO_2CH_3$	−16.2 (495)	+30.3 (295)
R= (*R*)-$SCH_2CH(NH_2)CO_2CH_3$, R^1= CH_3	+184 (495)	−171 (294)

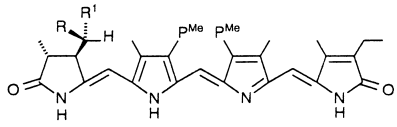

	$\Delta\varepsilon^{max}$ (λ^{max})	
104 DME	− 10.2 (640)	+ 7.7 (335)
R= CH_3, R^1= (*R*)-$SCH_2CH(NH_2)CO_2CH_3$	−98.6 (590)	+76.3 (348)
R= (*R*)-$SCH_2CH(NH_2)CO_2CH_3$, R^1= CH_3	+30.9 (590)	−27.5 (348)
R= CH_3, R^1=γ-Glu(O*Me*)-Cys-Gly(O*Me*)	+248 (590)	−420 (342)
R= γ-Glu(O*Me*)-Cys-Gly(O*Me*), R^1= CH_3	−300 (590)	+500 (347)

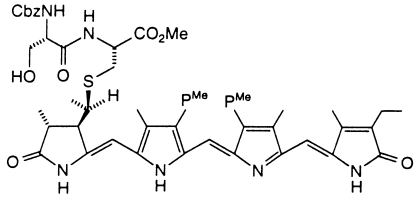

Δε = −51 (595), Δε = +100 (352) in $CHCl_3$

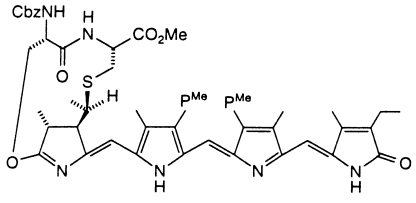

Δε = +82 (667), Δε = −134 (354) (Ref. 73)

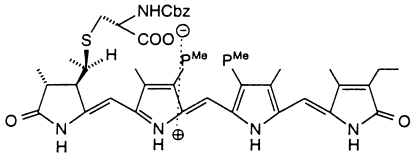

Δε = −35 (593), +52 (350),
−16 (275) in $CHCl_3$

(2*S*,3*S*,3^1*S*,Cys*R*)diastereomer
Δε = +38 (623), −56 (349),
+19 (273) in $CHCl_3$ (Ref. 74)

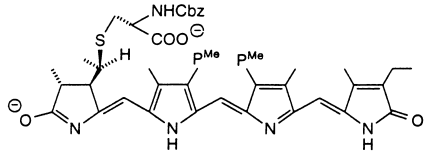

Δε = +41 (762), −32 (411)
−37 (361) in $CHCl_3$ (Ref. 75)

The chiroptical properties of a bridged 2,3-dihydrobilatriene-*abc* (**129**),[76] were determined. The bridge consists of (*S*)-lysine linking (3*S*)-acetic acid to the 12-propionic acid, and pigment **129** is thus predicted to be more flexible and ‘native-like’ than the N_{21}–N_{24} methano-linked etiobiliverdin (**44**) and isophorcabilin. The CD data were discussed in relation to the propensity of **129** to adopt helical (4*Z*, 10*Z*, 15*Z*, 5*sp*, 9*sp*, 14*sp*) or extended (4*E*, 10*E*, 15*Z*, 5*sp*, 9*ap*, 14*sp*) conformations, as in $CHCl_3$ and

hexamethyl phosphoric triamide (HMPT), respectively.[77] Several types of helical arrangements were considered to account for relatively weak CD observed (compare Δε for **129** vs Δε for **120**).[77]

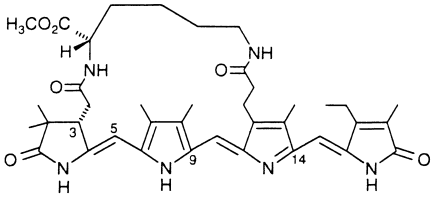

129

$\Delta\varepsilon^{max}$ (λ^{max})		
+ 18.5 (560)	- 29.0 (340)	in CCl_4
+ 14.2 (530)	- 8.9 (365)	in HMPT
- 13.1 (627)	+ 12.8 (528)	
	+ 6.1 (360)	in $CHCl_3$+TFA

Biliprotein chiroptical data prior to 1983 were included in a review by G. Blauer.[78] Similar to **129**, but in contrast to helical **115**–**125**, some 2,3-dihydrobilatriene-peptides from natural sources exhibited conformational heterogeneity other than that associated with helix enantiomerism. Four different chromopeptides (**130**–**133**) obtained from pepsin digestion of *Spirulina geitleri* C-phycocyanin as a mixture[79] or individually[80] showed rather different CD spectra at pH 2 and 8 for the folded or urea denaturated forms (Table 8). It was concluded that **130**–**133** existed not only in a helical but also in semi-extended[79] or non-uniformly twisted conformations, the latter as a consequence of hydrophobic and steric interaction or localized hydrogen-bonding between apoprotein and chromophore.[80] Without appropriate reference compounds, however, such use of CD data should be taken with caution.[44]

Table 8
Circular dichroism data in water for bilipeptides obtained following pepsin digestion of *Spirulina geitleri* C-phycocyanin

	$\Delta\varepsilon_{vis}$ [a]	$\Delta\varepsilon_{uv}$ [a]	$\Delta\varepsilon_{vis}$ [b]	$\Delta\varepsilon_{uv}$ [b]
130	- 5.8	+11.4	—	—
131	- 5.8	+13.1	+ 3.2	-3.3; +2.4
132	+16.2	-17.4	+20.3	-27.3
133	+24.8	-32.4	+23.1	-34.4

[a] pH 8, without urea; [b] pH 8, with 8 M urea.

Three distinct chromopeptides (**134**–**136**) were obtained by proteolytic degradation of phycoerythrocyanin.[81] The intense CE at ~680 nm followed by strong positive CE at ~340 nm in **134** were reminiscent of the CD spectrum obtained from the A-ring linked β-1 phycocyanobilin group of C-phycocyanin (**114**),[63,82] while the β-2 chain derived **135** did not share similarity with the corresponding C-phycocyanin pigment (**137**).[82] Trypsin and thermolysin digestion of *Synechococcus* 6301 C-phycocyanin yielded peptides **137** and **138**. The chromopeptide **138** was released from the α-subunit polypeptide chain of C-phycocyanin, whereas **137** originated from the β-chain which also contains **114**. The very different chiroptical properties of **114** and **137** (Fig. 10) provided the basis for the original proposal of a D-ring linkage in **137**,[82] but this was later corrected to the typical A-ring link[81] (with unknown absolute configuration).

134 Asn-Gln-Ala-Ala-Cys(**PCB**)-Ile-Arg
Δε~ -11 (680), Δε~ +7 (340)

135 Gly-Asp-Cys(**PCB**)-Ser-Gln
Δε~ -5 (680), $\Delta\varepsilon_{sh}$~ -4 (620)
Δε~ -4 (364), Δε~ +3 (310)

136 Cys(**PXB**)-Val-Arg
Δε~ -6 (604), Δε~ +8 (328)

137 Ile-Thr-Gln-Gly-Asp-Cys(**PCB**)-Ser-Ala
Δε~ +5(738), Δε~ -3(680), Δε~ +6(620)
Δε~ -3(523), Δε~ -6(370), Δε~ +7(310)

138 Cys(**PCB**)-Ala-Arg

PCB = phycocyanobilin chromophore as in **114**
PXB = biliviolinoid chromophore of unknown structure

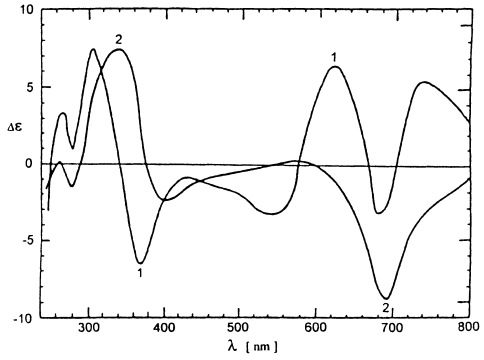

Figure 10. Circular dichroism spectra of aqueous TFA (10 mM) solutions of chromopeptides **137** (38.7 μM, Spectrum 1), and **114** (45.1 μM, Spectrum 2). Redrawn from Bishop et al.[82]

The unusual D-ring linkage was also proposed for phycoerythrobilins connected to small peptides (**140** and **141**), as well as for doubly linked **142**.[83] Such phycoerythrobilins were obtained by exhaustive enzymatic degradation of *Porphyridium cruentum* R-phycocyanin (β-chain, **140**) and B-phycoerythrin (β-chain, **141**) and were compared to **139** by CD spectroscopy.[66] All peptides **139**–**142** exhibited strong positive CEs in the visible region, which is characteristic for the (*R*) configuration at C(16) [or at C(4) in D-ring linked pigments], as shown in earlier synthetic studies.[62] Differences between A- and D-ring linked **103** peptides were observed in the UV region, where A-ring linked **139** showed a negative CE at 320 nm and a weak positive CE at 300 nm. However, both **140** and **141** had a positive CE at 300 nm of intensity almost equal to that of the long wavelength CE. Doubly-linked **142** showed CD features characteristic of both A- and D-linkage: a strong positive CE in the visible range, a negative CE at ~325 nm (attributable to A-ring linkage) and a positive CE at ~305 nm (attributable to D-ring thioether linkage).[83]

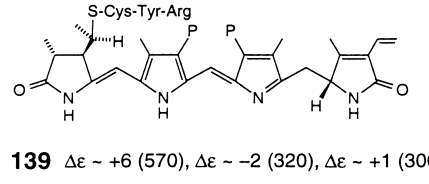

139 Δε ~ +6 (570), Δε ~ –2 (320), Δε ~ +1 (300)

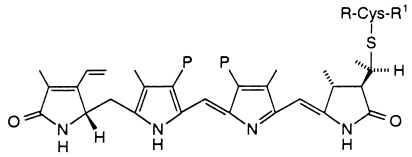

140 R= Gly-Asp, R^1= Ser-Ser
Δε ~ +6 (570), Δε ~ +2 (360), Δε ~ +6 (300)

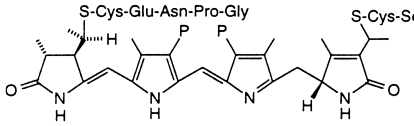

141 R= — R^1= Thr-Ser
Δε ~ +6 (570), Δε ~ +1 (350), Δε ~ +5 (300)

142 Δε ~ +13 (570), Δε ~ +2 (360), Δε ~ –2 (325), Δε ~ +4 (305)

The crystal structure of C-phycocyanins from the cyanobacterium *Mastigocladus laminosus* (2.1 Å resolution) and from *Agmenellum quadruplicatum* (2.5 Å resolution)[84] defined all three chromophores of the phycocyanobilin (**104**) type as having a stretched (4*Z*, 10*Z*, 15*Z*, *anti*, *syn*, *anti*) geometry interacting similarly with the protein, and the (2*R*, 3*R*, 3^1*R*) absolute configuration, confirming earlier conclusions.[61,63] Better agreement between the visible absorption calculated as λ^{max} α-508 nm, β-538 nm for this geometry and the experimentally estimated λ^{max} 595, 618, 624 nm[85,86] (as well as with the experiment CD spectrum[85]) was achieved when SCF-MO-CI calculations in the PPP approximation involved Van der Waals and coulombic interactions of the α-protein chain chromophore with neighboring aspartate, lysine, and arginine residues and assuming different tautomeric forms of propionic acid side chains and arginine.[87,88] This model showed also the greater rotatory strength variation with

charge heterogeneity in the polar protein microenvironment. The same type of calculations on the β-protein chain, however, indicated in addition contributions from exciton type interactions between both chromophores.[89] Evidence for such exciton coupling was revealed in biliprotein phycoerythrin 545 from marine cryptomonad *Rhodomonas lens* with a polypeptide structure $\alpha_2\beta_2$ where each α-polypeptide chain contained one covalently bonded cryptobilin 562 chromophore and each β-chain probably three covalently bonded phycoerythrobilin **103** chromophores. The native protein exhibited split CD CEs for the visible band: $\Delta\varepsilon_{565}^{max}$ −450, $\Delta\varepsilon_{533}^{max}$ +300, which was persistent on urea denaturation. The separated α- and β-polypeptide chains showed only positive CD CEs, and only the β-chain on refolding regained bisignate CD shape. A model involving intra-β-chain and inter-β(α)-chains exciton interactions was proposed to account for the observed CD data.[90] Two phycoerythrocyanin (PEC) fractions were isolated from the cyanobacterium *Westiellopsis prolifica* ARM36, and one of dissociated protein units resembled that of α-subunit in other PEC, but α-84 phycocyanobilin was replaced by phycoviolobilin chromophore.[81,91] This biliprotein showed photochemistry reminiscent of that of phytochrome in higher plants. The CD spectra changed upon irradiation with green (600 nm) or orange (500 nm) light. From these changes it was shown that 570 nm chromophore form had a positive CD roughly similar in magnitude and identical sign to the other phycobiliprotein chromophores in their native environment. By contrast, the CD of the 500 nm form was negative and decreased in amplitude.[92]

The blue-green chromopeptide phytochrome (P), the plant photosensory pigment, exists in two interconvertable forms: a physiologically inactive red absorbing 660 nm form (P_r) and a physiologically active far-red absorbing 730 nm form (P_{fr}).[93] The P_r form containing (15*Z*) chromophore **105** has a negative long wavelength CE and is fluorescent. The far-red P_{fr} form containing the (15*E*)[94] chromophore has a positive CD and is not fluorescent (Fig. 11).[95] Early absorption and CD measurements of small phytochrome between 203 K and 277 K, and comparison with Hückel MO calculations revealed the likely interconversion pathways between P_r and P_{fr} forms and their photochemical intermediates.[96] Evidence from chiroptical spectroscopy for these processes was also obtained by F. Thümmler and W. Rüdiger in 1983.[97] By following the CD spectral changes of a large phytochromobilin containing protein (**143**) (Table 9) they showed the $P_r \leftrightarrows P_{fr}$ phototransformation in presence of urea. This $Z \leftrightarrows E$ photoisomerization was observed and compared using CD spectroscopy with that of phycocyanin small peptide fractions containing a (*Z*) or (*E*) chromophore.[97] Native 124 kDa phytochrome from etiolated *Avena sativa* L. seedlings in its P_r form showed the same CD spectrum as degraded 118/114 kDa phytochrome (negative CE at ~660 nm and positive CE at ~360 nm). In contrast, the CD spectrum of the P_{fr} forms of 124 kDa and 118/114 kDa species differed, confirming that the NH_2-terminal polypeptide segment played a crucial role in chromophore-protein interaction in the P_{fr} but not in the P_r form. In the UV region (222, 209 nm maxima), the 124 kDa phytochrome exhibited a photoreversible difference between the CD spectra of P_r and P_{fr}, whereas no such difference was observed for 118/114 kDa fraction (Fig. 11). Thus, the N-terminus 6/10 kDa domain appeared to be at least one of the protein domains where the light-induced conformational change to higher α-helical contents accompanied $P_r \rightarrow P_{fr}$ phototransformation.[95]

The currently accepted view on the conformations of P_r and P_{fr} in the protein binding pocket is schematically[98] shown in Fig. 12. More recent, time-resolved absorption studies revealed the $P_r \rightarrow P_{fr}$ phototransformation kinetics, and the apparent life-times of five kinetic intermediates were estimated to be 7.4 μs, 89.5 μs, 7.6 ms, 42.4 ms, and at least 266 ms.[99] The steady-state CD spectra of phytochrome photointermediates trapped at 163 K were reported in 1988.[100] Transient CD spectra were measured at physiological temperature (283 K) by Kliger, Song and coworkers in 1992 by applying time-resolved CD spectroscopy (a useful new technique which is complementary to time-resolved absorption spectroscopy) to the $P_r \rightarrow P_{fr}$ phototransformation of native 124 kDa oat phytochrome in the 500–800 nm spectral region from 500 ns to 500 ms after the photolysis.[101] The difference between the 163 K and 283 K CD

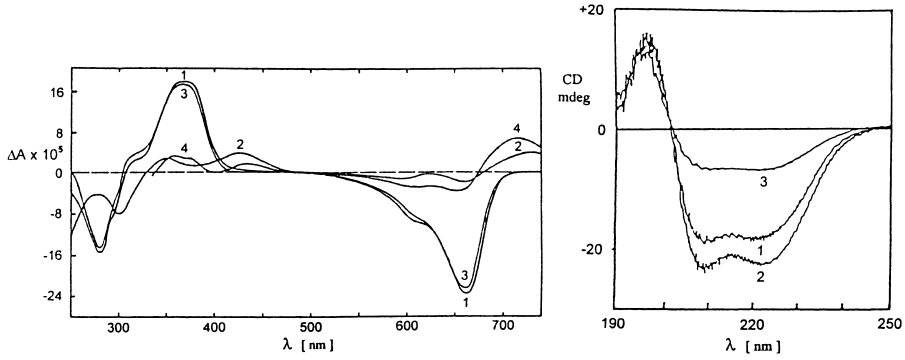

Figure 11. Circular dichroism spectra of phytochrome. Left: Visible–near-UV range, native 124 kDa P_r (Spectrum 1), P_{fr} (Spectrum 2) and degraded 118/114 kDa P_r (Spectrum 3), P_{fr} (Spectrum 4). Right: Far-UV range, native 124 kDa P_r before conversion to P_{fr} (Spectrum 1), P_{fr} (Spectrum 2), P_r after conversion from P_{fr} (Spectrum 3). All CD spectra were recorded in 0.1 M potassium phosphate pH 7.8 buffer at 293 K. Redrawn from Sommer and Song[95b]

Table 9
Circular dichroism data for phytochrome

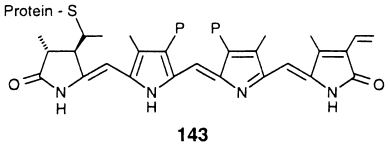

	$\Delta\varepsilon^{max}$ (λ^{max})				
P_r pH 7.7	−38.2 (665),	+45.0 (368),	−45.0 (286),	+6.4 (264)	
Bleached form	−3.2 (676),	+2.9 (580),	+7.1 (385),	−13.6 (286),	+12.9 (264)
P_{fr} pH 1.5 + urea	+19.3 (671),	+10.4 (440),	−18.2 (420),	−15.7 (380),	+25.7 (264)
P_r pH 1.5 + urea	+31.1 (682),	−17.1 (385),	−17.1 (360),	−10.4 (305),	+24.6 (264)

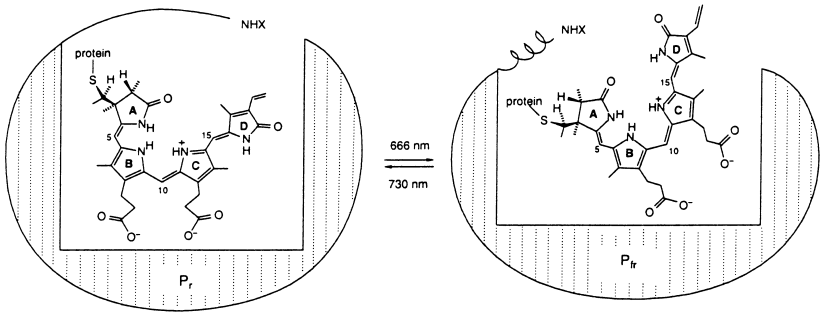

Figure 12. A possible mechanism for the phototransformation of phytochrome based on the isomerization at the C(15)–C(16) double bond in the primary photoprocess of P_r (right). The overall semiextended conformation of the D-ring is retained during the transformation by chromophore–apoprotein interactions. The model also incorporates the postulated orienting and the more exposed nature of the P_{fr} chromophore, as well as the increase of the α-helical folding of the N-terminus

data was attributed to a conformationally strained yet unrelaxed intermediate trapped at low temperature after the $Z \rightarrow E$ tetrapyrrole photoisomerization. These time-resolved CD studies in the visible region thus associated the early photointermediates with changes in interactions between the chromophore and charged and/or aromatic amino acid residues in the chromophore pocket.[101] To probe the time evolution of the N-terminal α-helix folding in late phytochrome photointermediates, time-resolved CD measurements were also performed in the far-UV 200–290 nm region.[102] The observed increase of P_{fr}

ellipticity at 220 nm was fitted to a single exponential function with decay rate of 113 ms, which allowed for identification of the photointermediate (life-time 42 ms) where the protein rearrangement occurred.[102]

As indicated above, alteration of the dipyrrin chromophore may switch the mechanism of optical activity. Removing the chromophore conjugation led to diminished CD found in a chlorophyll catabolite (**144**)[103] from enzymic breakdown of pheophorbide *a* due to the presence of perturbed symmetrical chromophores.

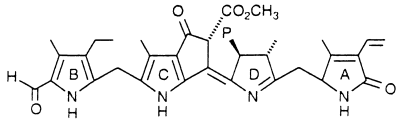

144

Relative Δε in H_2O		
sh + 0.60 (360),	+ 1.00 (328),	− 0.50 (282)
− 0.67 (238),	− 1.65 (205)	

7. Bilirubin and its chiral analogs

The dipyrrinone structural unit (**II**) occurs widely in nature and is found twice in the abundant, natural bile pigment of mammals, bilirubin-IXa (**145**). Bilirubin is produced in healthy adult humans at a rate of ~300 mg/day following catabolism of heme (Fig. 1). Its transport and metabolism are not governed simply by the functional groups in the molecule in their relative orientations but also by its three dimensional (3-D) structure of the pigment.[5,104,105]

4Z-Dipyrrinone

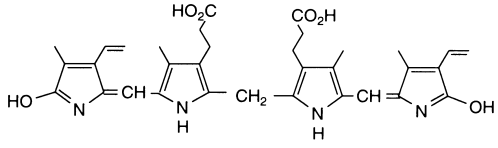

Bilirubin (Fischer, **1941**)[106]

The constitutional structure of bilirubin was proved long ago in a total synthesis by Fischer, Plieninger and Weissbarth.[106] Although Fischer's structure is consistent with many of the bilirubin's properties, e.g., a yellow color and solubility in dilute aqueous alkali, it is inconsistent with many other properties, such as its high oil–water partition coefficient,[105] its resistance to hepatobiliary excretion,[104] and — unusual for a carboxylic acid — its insolubility in aqueous sodium bicarbonate solution.[105] The reason for the apparent inconsistency is that Fischer's structure represents only the constitutional structure of the pigment, not its conformational or 3-dimensional structure. For bilirubin and its metabolism, the conformational structure has turned out to be of crucial importance. The first unequivocal information on bilirubin structure came from X-ray crystallographic analysis of the molecule in the solid: (i) a crystal obtained from diethyl ether:pyridine by Bonnett et al.;[107] the chloroform:methanol solvate in a crystal grown by LeBas et al.;[108] the bis-isopropylammonium salt crystallized by Manitto et al.;[109] and the crystalline mesobilirubin-IXα (**146**, where the vinyls in **145** are saturated to ethyls) by Sheldrick.[110] Both dipyrrinone chromophores in **145** and **146** are conjoined at and capable of independent rotation about the central C(10)–CH_2. Through such rotations the carboxyl group of one dipyrrinone is brought into sufficiently close proximity to

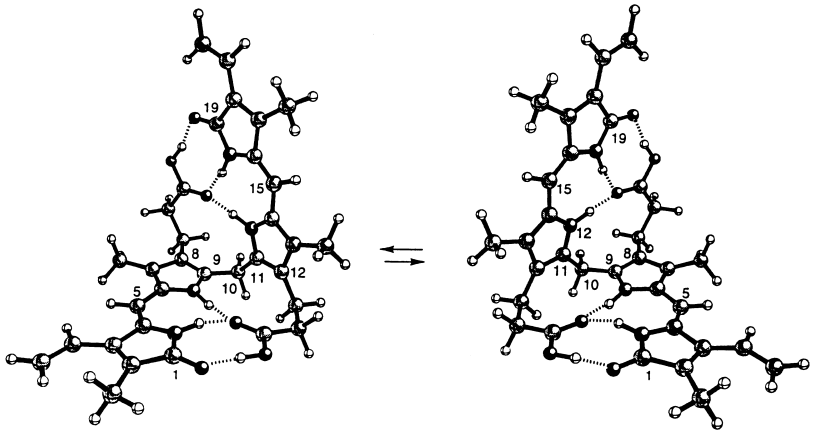

Figure 13. Ball and stick conformational representations for ridge-tile shape *M*- and *P*-chirality intramolecularly hydrogen-bonded interconverting enantiomers of bilirubin IXα. These conformers correspond to global energy minima on an energy hypersurface[2]

engage the other dipyrrinone's lactam and pyrrole moieties in a matrix of intramolecular hydrogen bonds (Fig. 13), thereby leading to two nonsuperimposable conformations.[111,112] These enantiomeric 'ridge-tile' shape conformations in the global energy minimum were consistently found in solid state and in solution.

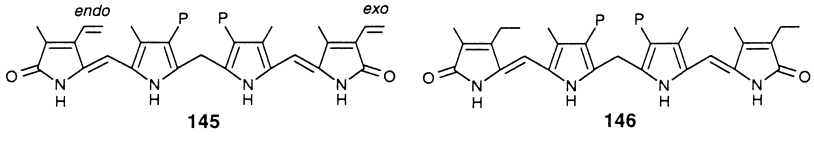

The two-mirror image conformations of Fig. 13 are undistinguishable by NMR. Manitto and Monti introduced one chiral center in **145** by addition of thiolacetic acid to the bilirubin C(18)-*exo*-vinyl group, thus rendering the conformers in Fig. 13 diastereomeric. The two singlets and two doublets (found at room temperature in the ^{1}H-NMR) of the C(18)–CH(CH_3)SCOCH_3 fragment coalesced at T_c=326 K,[33] and from this was calculated an activation barrier $\Delta G^{\ddagger}$=75 kJ mol[1]. In 1984 analysis and simulation of degenerated eight-proton spin systems of both propionic acid chains provided $\Delta H^{\ddagger}$=74.1±2.5 kJ mol^{-1}, $\Delta S^{\ddagger}$=−8.8±7.1 J mol^{-1} K^{-1} for **145** and $\Delta H^{\ddagger}$=72.4±1.3 kJ mol^{-1}, $\Delta S^{\ddagger}$=−12.6±3.8 J mol^{-1} K^{-1} for **146**.[113] A slightly lower activation barrier ($\Delta H^{\ddagger}$=82.4±5.9 kJ mol^{-1}, $\Delta S^{\ddagger}$=43.5±18.8 J mol^{-1} K^{-1}) was found for sterically congested α,α,α′,α′-tetramethylmesobilirubin-XIIIα by line shape analysis of the diastereotopic α-methyl groups ^{1}H-NMR signals.[114]

In the absence of an external dissymmetric agent, the enantiomeric *M*- and *P*-ridge-tile conformations of bilirubin and similarly substituted analogs are isoenergetic, equally populated and consequently, their equilibrated state is optically inactive. Any displacement of the equilibrium in Fig. 13 would lead to optical activity. Early chiroptical measurements were used to detect this phenomenon in solution generated by dynamic complexation processes through the intervention of non-covalently bound optically active perturbers such as proteins, chiral additives or solvents. All these cases are classified as induced optical activity[1] and will not be discussed in this review. Prior to 1987, only a few CD data of **145** with covalently attached chiral perturbers had been reported: (i) a synthetic bilirubin–HSA complex $\Delta\varepsilon^{max}_{470}$ ~ +3, $\Delta\varepsilon^{max}_{435}$ ~ −0.6, $\Delta\varepsilon^{max}_{390}$ ~ +6 at pH 4.5–7.5 buffer;[115] (ii) the δ-pigment $\Delta\varepsilon^{max}_{459}$ +9.9, $\Delta\varepsilon^{max}_{412}$=−2.4, $\Delta\varepsilon^{max}_{366}$=+3.1 at pH 7.3 buffer.[116] Regardless of the way a displacement of equilibrium (Fig. 13) is achieved, the CD spectra of **145** usually display two intense (to very intense, Δε >200) CEs flanking the

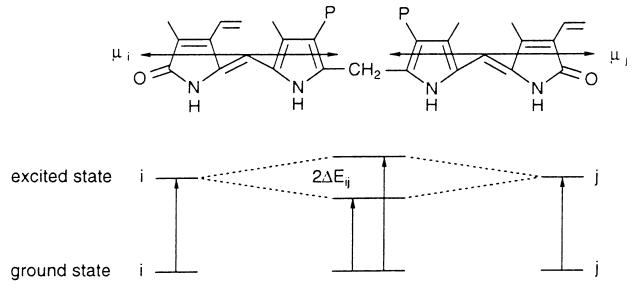

Figure 14. Arbitrary energy levels of the isolated dipyrrinone chromophore i (left), chromophore j (right) and their exciton coupled electronic system ij in bilirubin (middle)

dipyrrinone chromophores strongly allowed $\pi \rightarrow \pi^*$ transition, (ε_{420}^{max} ~30,000). These Cotton effects have opposite signs and almost equal intensity (rotatory strength). The most probable mechanism of bilirubin optical activity was clarified in 1987, and it is valid for all cases described below.[117]

The dipyrrinone chromophore (**II**) of **145** is planar and thus inherently symmetric. Chiral perturbation is not a likely mechanism because compounds equivalent to one half of **145** or **146**, the xanthobilirubic acids, such as **178** and **179**, exhibit only weak and monosignate CD under the same conditions. The CD spectrum of **145** is not simple sum of its component dipyrrinone CD spectra. The bisignate nature of bilirubin CD spectra is typical of excited state interaction in weakly coupled electronic systems, e.g., exciton coupling.[118,119]

In the bilirubin ridge-tile conformation, where the interplanar dihedral angle between the dipyrrinones is ~100°, the dipyrrinone chromophores have only a small π-orbital overlap but interact through their locally excited states — electrostatic interaction of the local electric dipole transition moments. The polarization of this transition moments has been calculated in the PPP approximation[34] and estimated from linear dichroism measurements[120] to be parallel to longitudinal axis of the planar conjugated π-system. The mutual orientation of the participating electric dipole transition moments can be attractive or repulsive, thus the dipyrrinone–dipyrrinone intramolecular exciton interaction produces two non-degenerate excited states separated by Davydov splitting energy gap $2\Delta E_{ij}$ (Fig. 14). When observed by UV–vis spectroscopy, the two electronic transitions overlap to give a broadened long wavelength absorption band characteristic of bilirubins. In the CD spectra, however, exciton theory[119] predicts that the two transitions will be oppositely signed, and thus typical bisignate CEs are seen for **145**. As a result of band overlap in the CD spectra, there is considerable cancellation in the region between the band centers, with the net appearance of CE maxima displaced from the actual λ_{max} of an isolated dipyrrinone. More importantly, from the theory for a general case, and as applied to bilirubin,[117] the signed order of these CEs is related to the absolute sense of helicity between the interacting dipoles, or so called exciton chirality. A left-handed sense results in a negative exciton couplet CD (long wavelength negative CE followed by positive short wavelength CE) and a right-handed transition moments disposition is expressed by positive exciton couplet CD (positive long wavelength CE and negative short wavelength CE). Thus, in the case of bilirubin analogs, as opposed to twisted dipyrrins, the exciton CD provides a non-empirical correlation[119] between CE signs and absolute conformation, i.e., the two crucial torsional angles around C(10)–CH_2 signs. The importance of chiroptical spectroscopy for conformational analysis in bilirubins comes from the potentially enormous exciton coupling CE magnitudes ($\Delta\varepsilon$ >200) associated with either *M*- or *P*-conformer alone. Only a small displacement from a 1:1 equilibrium in Fig. 13 can generate intense CD. For example, a free energy difference between diastereomeric *M*- and *P*-helical **145** derivative of 4.2 J mol^{-1} would correspond to 50.05:49.95 equilibrium or 0.1% helical excess which would result in easily detectable CE of $\Delta\varepsilon$ ~0.2.

Table 10
Circular dichroism spectral data for bilirubin esters and amides in benzene solvent

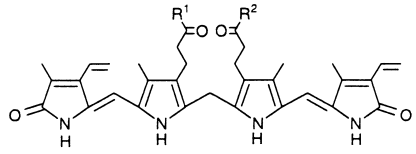

			$\Delta\varepsilon^{max}$ (λ^{max})	
147	R^1=R^2=	(*R*)-OCH(CH_3)CH_2CH_3[a]	- 1.5 (450)	+ 1.1 (400)
		(*S*)-OCH(CH_3)C_6H_5	+ 6.7 (455)	- 2.4 (400)
		(*R*)-OCH(CH_3)$CO_2C_2H_5$[a]	- 3.5 (450)	+ 2.1 (400)
		(*S*)-NHCH(CH_3)CH_2CH_3	- 16.3 (455)	+ 1.2 (405)
148		(*S*)-NHCH(C_2H_5)C_6H_5	+ 75.3 (458)	- 53.2 (405)
149		Ala-O*Me*	+ 57.9 (450)	- 40.0 (401)
150	R^1=H,[b] R^2=	(*R*)-OCH(CH_3)CH_2CH_3[a]	- 21.2 (450)	+ 12.6 (405)
		(*S*)-OCH(CH_3)C_6H_5	+ 25.8 (450)	- 13.6 (400)
		(*R*)-OCH(CH_3)$CO_2C_2H_5$[a]	- 18.1 (453)	+ 13.9 (405)
		(*S*)-NHCH(CH_3)CH_2CH_3	- 4.0 (470)	+ 2.0 (415)
151		(*S*)-NHCH(C_2H_5)C_6H_5	+ 46.5 (460)	- 35.5 (420)
152		Ala-O*Me*	+ 27.5 (452)	- 20.2 (402)
		Trp-O*Me*	+ 20.8 (460)	- 12.3 (410)

[a] Obtained from (*S*)-tosylates and bis-NBu_4 salt of **145** via S_N2 reaction; [b] Unseparated mixtures of 8- and 12-isomers.

The chiral induction due to remote stereogenic center(s) as in mono- and diesters of **145** with (2*R*)-butanol[116,121] and ethyl (*R*)-lactate[116] led to only a slight predominance of the *M*-helical diastereomer over the *P*-, and with (1*S*)-phenylethanol[122] — of the *P*- over the *M*-isomer (Table 10). The preferred conformation of monoesters like **150** was thought to be similar to that of the parent diacid **145**, with partially retained intramolecular hydrogen bonding from unesterified side chain. Such stabilization provided an explanation for the stronger CEs seen in monoesters vs diesters, (cf. **150** vs **147**). The 5–10-fold weaker CD of diesters was attributed to mutual cancellation of contributions from a multiplicity of conformations of monomeric and aggregated species. The situation was just opposite for **145** mono- and bis-amides (Table 10). For example, the CD of bis-amide **148** was much stronger than that of the corresponding mono-amide **151**[122] due to higher *P* stabilization through intramolecular hydrogen bonds offered by propionamide NHs. Additional distant ester carbonyl groups, as provided in alanine derivatives **149** and **152** did not seem to participate as an acceptor. Here also the chiral residues of bis-amide **149** reinforce the *P*-helicity selection to give more intense CD than mono-amide **152**.[116]

Three isomeric *N*-acetyl-(*R*)-cysteine adducts, with attachment at the 18-*exo*-vinyl group of **145**, showed remarkably large CD CEs ($|\Delta\varepsilon|$ ~40–60) in dimethyl sulfoxide (DMSO), a solvent known to disrupt the intramolecular hydrogen bonds network, and the CE sign also depended on the newly created C(18^1) chiral center configuration.[123]

Prior to 1991, bilirubin had never been resolved into pure *M*- or *P*-helical enantiomers and conformed experimentally with the way helical excess corresponded to earlier measured ICD. In 1991, Lightner et al. proposed a novel way to displace $M \leftrightarrows P$ equilibrium of Fig. 13 using intramolecular steric effects generated by methyl substitution on the C(8) and C(12) propionic acid α- or β-carbons.[124,125] Close inspection of a space-filled molecular model for the minimum energy *P*-helical enantiomer (Fig. 15) hinted that the α-pro-*S* hydrogens (but not the α-pro-*R*) are brought into close non-bonded contact with C(7)/C(13) methyl groups, and the β-pro-*S* hydrogens (but not the β-pro-*R*) lie in close proximity to the C(10)–CH_2. Methyl groups replacing these α-pro-*S* or β-pro-*S* hydrogens would seek the least hindered

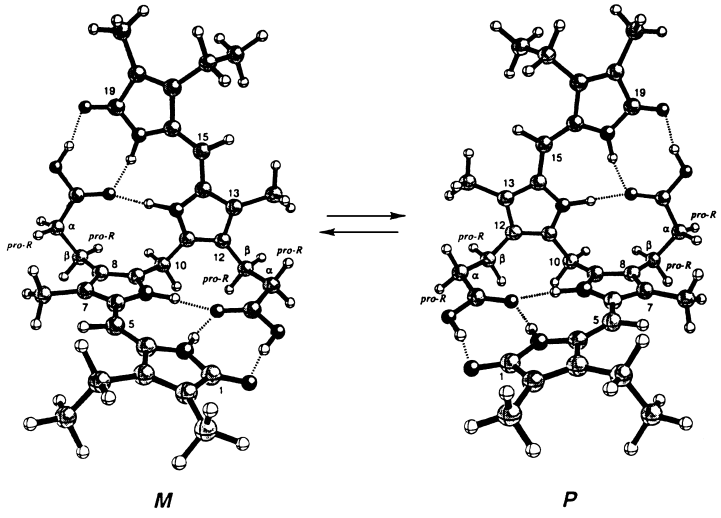

Figure 15. Ball and stick models of folded intramolecularly hydrogen-bonded mesobilirubin-XIIIα. The (pro-*R*) α-hydrogens are sterically compressed into the CH_3 groups at C(7) and C(13), and the (pro-*R*) β-hydrogens are sterically crowded by the $–CH_2–$ at C(10) in the *M*-helicity conformation. The pro-*S* hydrogens are sterically crowded in the *P*-helicity conformation. Replacing the pro-*R* hydrogens by CH_3 groups drives the equilibrium toward *P*, and replacing the pro-*S* by CH_3 groups drives it toward *M*. However, replacing one pro-*R* and one *pro-S* hydrogen by CH_3 gives a *meso* diastereomer (*R*,*S*) that can adopt either the *M* or the *P* conformation while leaving one propionic acid ineffectively hydrogen bonded

positions. Assuming that the integrity of the intramolecular hydrogen bonds matrix is maintained, which is of utmost importance for the success of this allosteric model, steric buttressing between C(7)/C(13) and (α*S*,α′*S*)-methyl groups or between C(10)–CH_2 and (β*S*,β′*S*)-methyl groups will destabilize the *P*-helical diastereomer and force the pigment to adopt an *M*-helical ridge-tile conformation. On the other hand, (α*R*,α′*R*)- or (β*R*,β′*R*)-methyl substitution will destabilize the *M*-helical conformer and force the pigment to adopt the *P* conformation. However, when the configurations in the propionic acid chain are not the same, as in the (α*R*,α′*S*)- or (β*R*,β′*S*)-dimethyl *meso* diastereomers, equivalent destabilizing steric interactions are introduced into both the *M*- and *P*-conformers. And this is expected to produce pigments whose one propionic acid is tightly intramolecularly hydrogen-bonded, but the other chain cannot fit comfortably and its COOH group is left relatively non-involved in intramolecular H-bonding, thereby increasing the pigment's polarity.

Synthetically more easily accessible (α,α′)- and (β,β′)-dimethylmesobilirubin-XIIIα were synthesized and both compounds were found to consist of pairs of diastereomers with large polarity differences. They were separated chromatographically, and the NMR spectroscopy pointed to C_2-symmetry for the nonpolar and C_s-symmetry for the polar diastereomer — the first sign of success of the allosteric model. The nonpolar (α,α′)-dimethylmesobilirubin-XIIIα isomer was resolved by chromatography on quinine modified silica gel or on a larger scale, by enantioselective binding to HSA in aqueous buffer and successive $CHCl_3$ extractions.[125] The initial $CHCl_3$ fractions were enriched in the *P*-helical enantiomer, and the last with *M*-helical (**153**) showing that **153** was bound to HSA more tightly (Fig. 16). The last somewhat contradicted earlier findings for natural bilirubin–HSA complexes.[126] The absolute configuration (α*S*,α′*S*) of **153** was assigned from $^1H\{^1H\}$-NOE on the corresponding bisamide from (*S*)-α-methylbenzylamine[125] and later reconfirmed by synthesis.[127] Optically pure (β,β′)-dimethylmesobilirubin-XIIIα (**154**) was obtained from an enantiomerically resolved monopyrrole precursor whose absolute configuration (*S*) was determined by X-ray crystallographic analysis relative to brucine.[128] Thus, **154** had (β*S*, β′S) configuration. Both **153** and **154** exhibited very intense negative

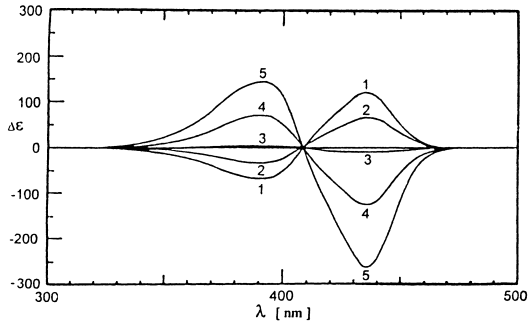

Figure 16. Circular dichroism spectra of the successive 100 mL $CHCl_3$ extracts of 100 mL of an initially 1:2 mole/mole aqueous solution of HSA (2.20×10^{-4} M) and racemic α,α′-dimethylmesobilirubin-XIIIα (4.35×10^{-4} M) (Spectrum 1, *ent*-**153** → Spectrum 5, **153**). Redrawn from Puzicha et al.[125]

Table 11
Circular dichroism data for (α*S*,α′*S*)-dimethyl and (β*S*,β′*S*)-dimethyl-mesobilirubins, in chloroform solution

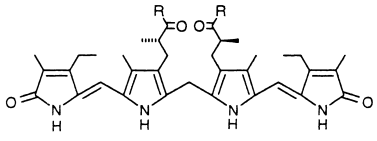

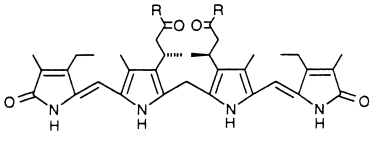

		$\Delta\varepsilon^{max}(\lambda^{max})$		$\Delta\varepsilon^{max}(\lambda^{max})$
153	R=OH	−251 (436) +142 (391)	**154** R=OH	−337 (434) +186 (389)
155	R=OCH_3	−19.7 (426) +11.8 (375)	**156** R=OCH_3	−131 (416) +63 (376)
	R=$O^-N^+(CH_3)_4$	−194 (438) +130 (394)	**157** R=NH_2	−403 (429) +216 (385)
			158 R=$NHCH_3$	−348 (431) +187 (386)
			159 R=$N(CH_3)_2$	+106 (416) −70 (375)

exciton chirality CD (Table 11) corresponding to *M*-helical conformer in complete agreement with the above arguments on allosteric action of the extra methyl groups and in support of the importance of intramolecular conformation stabilizing forces due to a hydrogen bonds network.[2,125,128]

If the intramolecular hydrogen bonds network of diacids **153** or **154** is disrupted or incomplete, as in the corresponding dimethyl esters **155** and **156**, then α,α′-dimethyl substituted rubin **155** exhibited very weak CD due to the presence of various conformations in solution, some being intermolecularly H-bonded dimers,[129] while the β,β′-dimethyl substituted analog **156** retained a strong preference for the *M*-helical shape. The CD intensity of **156** dropped ~60% vs **154** in $CHCl_3$ solvent and even more in polar or hydrogen-bonding solvents.[130] The CD spectra clearly indicated that intramolecular hydrogen bonding remained a powerful force in the *M*-diastereoselection in dianions of **153**[131] and **154**[128] even in aqueous solution. The primary (**157**), secondary (**158**), and tertiary (**159**) bis-amide derivatives of **154** provided additional evidence for the importance of a hydrogen bond donor sites in C(8)/C(12) side chains in order to achieve effective conformational stabilization.[132] While **157** and **158**, which have such sites showing higher or equal CD magnitudes to **154**, respectively, the tertiary bis-amide **159** lacking such donor sites exhibited CD spectra similar to that of diester **156**, in the sense that the CEs were drastically solvent-dependent. In solvents with low dielectric constant like benzene or 1,4-dioxane the CD of **159** exhibited the same CE signs but weaker CEs than that found in **154**, and the CE signs unexpectedly reversed in $CHCl_3$ or solvents with high dielectric constant (Fig. 17).[130,132] The CD spectral data of all homochiral mesobilirubin analogs **153**–**159** were interpreted not only from exciton coupling theory but by NMR spectroscopy (characteristic chemical shifts, spin–spin couplings and $^1H\{^1H\}$-NOE experiments) and

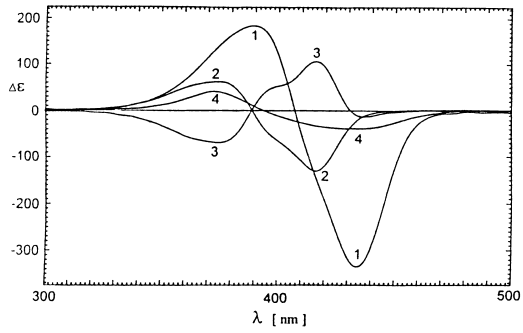

Figure 17. Circular dichroism spectra of $CHCl_3$ solutions of (β*S*,β′*S*)-dimethylmesobilirubin-XIIIα (**154**, Spectrum 1), its dimethyl ester **156** (Spectrum 2), bis-*N*,*N*-dimethylamide **159** (Spectrum 3), and bis-((*S*)-*i*-butyl) analog **164** (Spectrum 4)

Table 12
Circular dichroism data for acid-lengthened bilirubin analogs in $CHCl_3$ solvent

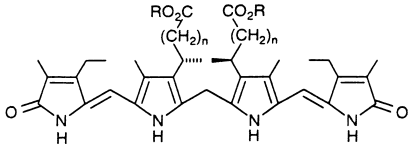

		$\Delta\varepsilon^{max}$ (λ^{max})	
R=H	n=2	+99.0 (441)	−68.7 (398)
	n=3	−88.1 (430)	+47.8 (386)
	n=4	−12.3 (434)	+82.0 (393)
	n=5	−88.9 (443)	+116.6 (395)
R=CH_3	n=2	−103.2 (413)	+68.8 (371)
	n=3	−20.5 (438)	+20.2 (371)
	n=4	−34.0 (429)	+40.5 (371)
	n=5	−38.1 (435)	+46.1 (372)

by molecular mechanics and dynamics calculations, which collectively serve as powerful tools in the elucidation of conformation.

Enantiomerically pure analogs of **154**, with propionic acid groups lengthened systematically to heptanoic acid, were synthesized and examined to explore how the alkanoic acid chain length influenced the conformational equilibrium of Fig. 15 and intramolecular hydrogen bonding. All homologs with acids longer than propionic acid exhibited much weaker CEs than **154** (Table 12), pointing to the optimum as the natural acid chain length. Negative exciton chirality CD spectra were found for all rubins and their corresponding dimethyl esters, except butanoic acid. The butanoic acid derivative had an inverted exciton chirality due to a change in the relative orientation of the component dipyrrinone chromophores and their long wavelength electric transition moments.[133]

In a search for the maximum allosteric action of α- and β-methyl groups, two tetramethyl substituted analogs **160** and **161** were designed and synthesized to probe their influence on conformational preference by CD spectroscopy. The absolute configuration of a key precursor of **161** was determined by X-ray crystallographic analysis.[134] When the methyl perturbers acted synchronously as in (α*S*,α′*S*,β*S*,β′*S*)-**160** the CE intensities were 70–90% of those seen in **154**, thus indicating that the conformational equilibrium of Fig. 15 is already displaced completely toward *M* in **154**. The data also reveal that any conformational reinforcement due to the additional α*S* and α′*S* methyl groups is not only redundant but is probably offset by the introduction of a new *gauche* butane interaction between the α- and β-methyls. When the methyl perturbers were in opposition as in (α*R*,α′*R*,β*S*,β′*S*)-**161**, then the steric influence of both (α*R*)-methyl

groups dominated, and a net positive exciton chirality was observed in nonpolar solvents. However, the dominance was not as effective in more polar solvents, such as CH_3OH, where β-methyls seemed to dominate. In such solvents, the CD spectra were more complex, as if multiple species were present.[135]

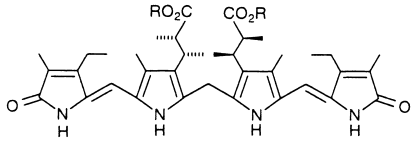

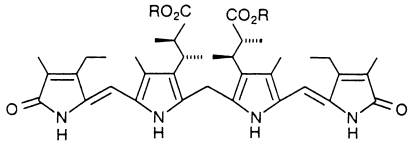

		$\Delta\varepsilon^{max}$ (λ^{max})		$\Delta\varepsilon^{max}$ (λ^{max})
160	R=H	−314 (436) +193 (390) $CHCl_3$	**161** R=H	+204 (433) −118 (388) $CHCl_3$
		−155 (432) +103 (388) CH_3OH		−21 (430) +34 (384) CH_3OH
	$R=CH_3$	+34 (410) −26 (370) $CHCl_3$	$R=CH_3$	−91 (427) +99 (369) $CHCl_3$
		−28 (417) +18 (376) CH_3OH		−29 (426) +22 (382) CH_3OH

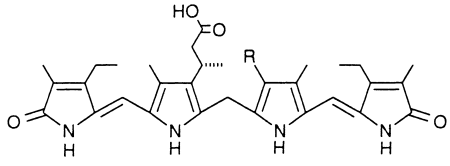

		$\Delta\varepsilon^{max}$ (λ^{max}) in $CHCl_3$			
162	$R=CH_2CH_2CH_3$	−178	(424)	+115	(379)
163	R=(*S*)-$CH(CH_3)CH_2CO_2CH_3$	−238	(422)	+153	(380)

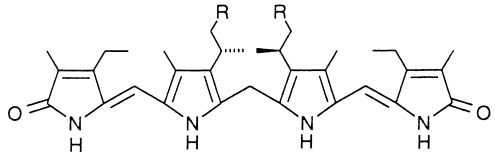

		$\Delta\varepsilon^{max}$ (λ^{max}) in $CHCl_3$			
164	$R=CH_3$	−40.1	(433)	+42.2	(373)
165	$R=CH_2OAc$	−58.3	(416)	+39.3	(373)
166	$R=CH_2NHAc$	−73.7	(419)	+50.4	(376)

It was recently found that only a single propionic acid chain, with (β*S*)-methyl substitution as in **162**, was sufficient for the diastereoselection of *M*-folded ridge-tile conformation.[136] A second (β′*S*) chiral center in a methyl propionate chain, as in the monoacid **163**, reinforced this enantioselection and increased the CE magnitude over that of dimethyl ester **156**. However, the CEs of **162** and **163** still remained weaker than those of diacid **154**, thus showing the partial absence of some intramolecular hydrogen bonds due to one ester residue.[130,136] Three mesobilirubin pigments **164**–**166** lacking carboxylic groups still exhibited moderately strong negative exciton chirality CD.[137] The correspondingly low diastereoselectivity for the *M*-helical isomer was exclusively derived from the pigment's simply adopting

a shape that minimized intramolecular nonbonded steric interactions. Thus, the CD of **164** (Fig. 17) might be viewed as a backdrop from which a 10-fold higher CD magnitude is accessed when the full complement of intramolecular hydrogen bonds acts to stabilize the conformation of **154**. The increased CD intensity of **165** and **166** vs **164** appeared to be linked to the ability of both **165**, and especially **166**, to participate in minimal intramolecular hydrogen bonding.[137]

Diastereomers of **153** and **154**, with opposite absolute configuration at the chiral centers [as in (α*R*,α′*S*) or (β*R*,β′*S*)] possess a symmetry plane and are achiral (*meso* type). However, with the (*R*) configuration at an α-carbon and an (*S*) at the β (or vice versa), the rubins are no longer achiral. Such asymmetrically substituted analogs (**167** and **168**) were obtained by the synthetic route outlined in Scheme 13, and their CD spectra were investigated.[127] *p*-Chloranil-promoted oxidative reaction of racemic dipyrrinone **172** and enantiomerically pure dipyrrinone **173** led to a mixture of self-coupled mesobiliverdin products **169** and **171**, and a mesobiliverdin product of cross-coupling **170**. The last being a monoacid was readily separated by chromatography from the diester **169** and the diacid **171**, and it was found by NMR to consist of two diastereomers. Purified **170** was saponified and reduced to a mixture of mesobilirubins, which had very different polarity and were easily separated, properties in accord with models based on non-bonded steric repulsions. In fact, this sequence (Scheme 13) constitutes an example of a classical optical resolution to 100% ee of **172** via covalent diastereomers **167** and **168** using **173** as the chiral auxiliary. The less polar (α*S*,β′*S*) diastereomer **167**, where both α- and β′-methyl substituents act in concert to displace the conformational equilibrium of Fig. 15, showed a very strong negative exciton chirality CD characteristic of the *M*-helicity.[127] The CE intensities of **167** corresponded nicely to those found for the **153** and **154** analogs. And as with **153** and **154**, they too were only slightly affected by solvent polarity, except for DMSO. In the more polar (α*R*,β′*S*) diastereomer **168**, the (α*R*)-methyl group prefers *P*-helicity conformer but the (β′*S*)-methyl group fits comfortably in the *M*-helicity conformer. The competition is dominated by the (α*R*) methyl, as **168** exhibited an intense positive exciton chirality CD, consistent with the equilibrium of Fig. 15 being displaced toward the *P*-helicity conformer. The CEs of **168** were considerably weaker and much more susceptible to decrease with increasing solvent polarity. These CD and extensive $^{1}H\{^{1}H\}$-NOE experiments on **167** and **168** suggested that, on balance, the steric influence of the (α*R*)-methyl group, as in **161**, counteracted and dominated that of the (β′*S*)-methyl substituent when they were in opposition in **168**.[127]

A chemical correlation of the tetrapyrrole helicity in biliverdins and bilirubins was first shown by Falk et al. Thus, sodium borohydride or sodium dithionite reduction of biliverdin **40** bound to apomyoglobin afforded bilirubin **145** bound to apomyoglobin:[138] *P*-helical bound **40** [ICD +43 (700), −63 (380) in H_2O][49] afforded *P*-helical bound **145** [ICD +23 (470), −15 (395) in H_2O].[138]

Krois and Lehner[52,55] have described bilirubin model compounds (**174**–**176**) which are forced to adopt a flattened porphyrin-like conformation and were obtained by $NaBH_4$ reduction of biliverdins **91**–**95**. They determined the barrier for $M \leftrightarrows P$ interconversion by kinetic measurements following the optical activity decay of partially resolved **174**, **175** and **176**: $\Delta G^{\ddagger}$=78.7, 77.8, 91.5 kJ mol^{-1} (at 266 K), respectively.[52] Owing to the low $M \leftrightarrows P$ barriers in **174** and **175**, the corresponding helical excess could not be determined, and only the initial CD data of partially resolved **174** and **175** were reported. Vapor pressure osmometry and UV–vis spectroscopy measurements suggested self-association, similarly to that in bilirubin **145** dimethyl ester: for the dimethyl esters **175** and **176** with dimerization constant K_{dim}=420–55,700 l mol^{-1} or oligomerization (i=5) with equal microscopic association constants K_i=240 l mol^{-1}. Various helical arrangements were discussed in this relation.[52]

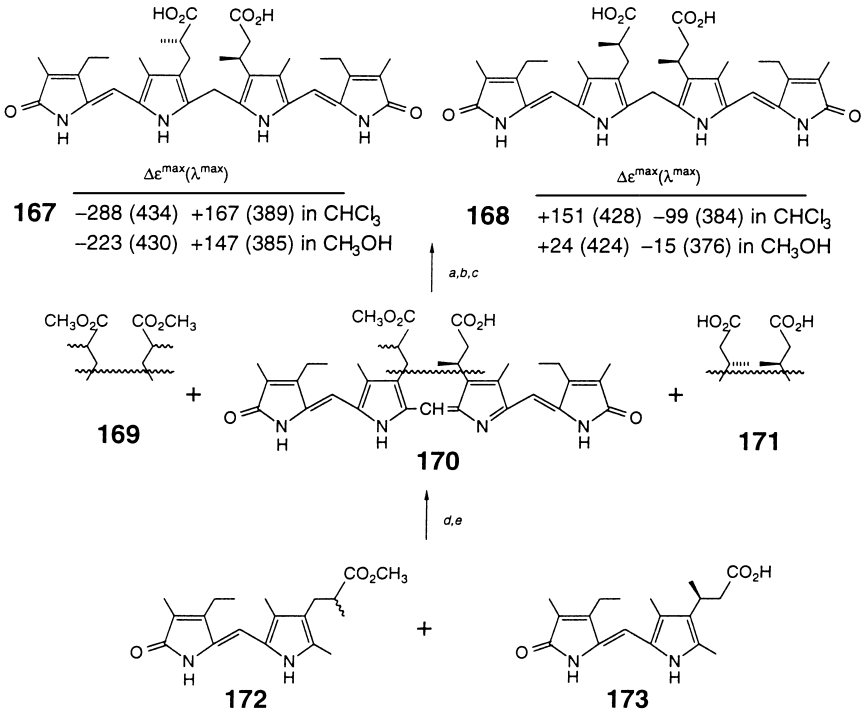

[a] $NaOH/H_2O$, then HCl. [b] $NaBH_4$, CH_3OH, THF, then CH_3CO_2H. [c] Chromatographic separation of **167** from **168**. [d] *p*-Chloranil, HCO_2H. [e] Chromatographic separation of **170** from **169** and **171**.

Scheme 13.

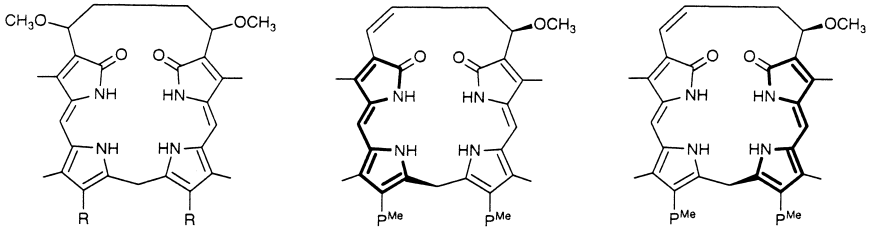

			$\Delta\varepsilon^{max}$ (λ^{max})		$\Delta\varepsilon^{max}$ (λ^{max})
174	R = $CH_2CH_2CO_2H$	(*M*,1′*R*)	−215.6 (444)[a]	(*P*,1′*R*)	+192.3 (446)[b]
			+253.5 (384)		−250.2 (386)
175	R = $CH_2CH_2CO_2CH_3$	**176A** (*M*,1′*S*)	−196.9 (447)[a]	**176B** (*P*,1′*S*)	+219.6 (444)[b]
			+256.3 (387)		−257.7 (385)

[a,b] in CH_3OH at 273 K; interchangeable Δε values since the absolute configuration at the chiral center was not known.

Chemical correlation of tetrapyrrole helicity of biliverdins and bilirubins was also shown from the conversion of verdin **94B** into rubin **176B** — the *P*-helical verdin **94B** with a positive long wavelength 625 nm CE gave a rubin with positive exciton chirality CD (Fig. 18).[55] The CD spectra of **176A** and **176B** were rather similar in shape to those of **154** with the major difference being the relative band widths. In **176**, the shorter wavelength band was narrower and had a higher Δε. This is remarkable considering the different conformations: flattened helical for **176** and folded ridge-tile for **154**,[128] and the correspondingly very distinct UV–vis spectra.[52,55]

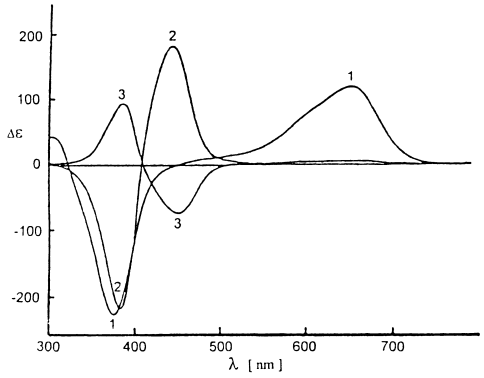

Figure 18. Circular dichroism spectra of CH_3OH solutions at 283 K of flattened helical biliverdin **94B** (Spectrum 1), bilirubin **176B** after completion of $NaBH_4$ reduction (15 min, Spectrum 2), and **176B** after completion of equilibration (3 h, Spectrum 3). Redrawn from Krois and Lehner[55]

8. Bis-dipyrrinones

The dipyrrinone chromophore (**II**) has been used in CD studies on exciton coupling in model mono and diesters of (1*R*,2*R*)-cyclohexanediol and compared to *p*-(dimethylamino)benzoate chromophore.[139] While the latter has an electric dipole transition moment colinear with C*–O bond, and rotations of the chromophore do not change the exciton chirality; the dipyrrinone transition moment vector has an oblique orientation to the carbonyl–pyrrole bond, and rotations around this bond could change the exciton chirality as has been observed for **177** in different solvents (Fig. 19).

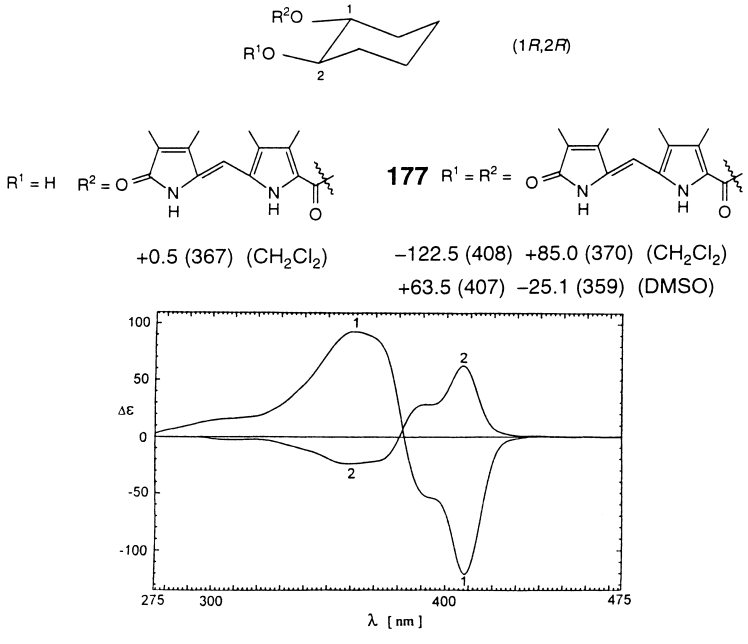

Figure 19. Circular dichroism spectra of the bis-dipyrrinone **177** in CH_2Cl_2 (Spectrum 1) and DMSO (Spectrum 2) solutions

The amides of xanthobilirubic acid (the chromophore of mesobilirubin, **146**) with (*R*) and (*S*)-phenyl- (**178**) and 1-naphthylethylamines (**179**) have been synthesized and found to exhibit moderate monosignate CD in DMSO, but stronger bisignate CD in $CHCl_3$ solvent.[140] In contrast, their CEs in DMSO were typical of inherently symmetric planar dipyrrinone chromophore perturbed by dissymmetric actions

from the amine chiral center. The CD in nonpolar solvents reflected a superposition of contributions from monomeric (monosigned CE) and dimeric, presumably planar species. The latter, hydrogen-bonded dimers were reminiscent of bilirubin intramolecular exciton system in producing bisignate CD curves, which originated, however, from intermolecular exciton splitting.[140]

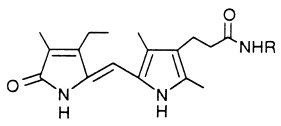

		$\Delta\varepsilon^{max}$ (λ^{max})
178	R = (*R*)-CH(CH_3)C_6H_5	-1.3 (413) (DMSO)
		+1.3 (446) -3.1 (402) ($CHCl_3$)
179	R = (*R*)-CH(CH_3)-1-Naphthyl	-1.7 (413) (DMSO)
		+2.0 (447) -5.2 (404) ($CHCl_3$)

Similar planar traditional dimers were responsible for the optical activity of the methyl esters corresponding to **180**–**186**. They showed simply low optical rotations and diminishingly small noise-level CD. In striking contrast, free acids **180**–**186** exhibited strong CD originating from intermolecular exciton interaction in nonpolar solvents which vanished in polar solvents (Fig. 20). A new type of π-stacked 3D dimer (Fig. 21), where the carboxylic acid group is tethered through a network of intermolecular hydrogen bonds to the second dipyrrinone lactam and pyrrole units was proposed to explain the chiroptical and NMR data.[134,141]

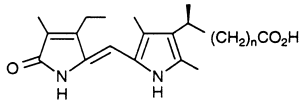

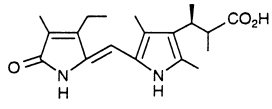

		$\Delta\varepsilon^{max}$ (λ^{max}) in CCl_4	
180	n=1	-25.0 (435)	+12.0 (392)
			+0.4 (388) (CH_3OH)
181	n=2	-7.2 (441)	+11.3 (401)
182	n=3	-41.9 (430)	+24.5 (393)
183	n=4	+10.0 (429)	-3.7 (389)
184	n=5	-11.4 (428)	+6.5 (393)

	$\Delta\varepsilon^{max}$ (λ^{max}) in CCl_4	
185 (α*R*)	-6.7 (428)	+6.8 (392)
186 (α*S*)	-33.0 (437)	+17.3 (396)

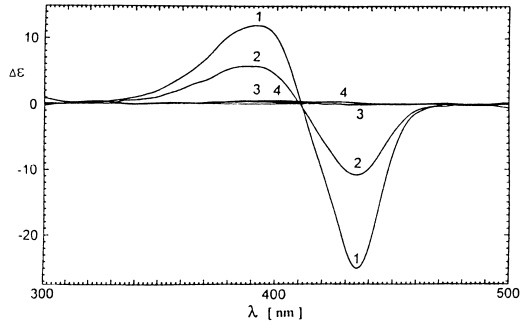

Figure 20. Circular dichroism spectra of (β*S*)-methylxanthobilirubic acid **180** in CCl_4 (Spectrum 1), $CHCl_3$ (Spectrum 2), CH_3OH (Spectrum 3), and its methyl ester in CCl_4 (Spectrum 4)

9. Concluding comments

The optical activity of linear tetrapyrrole pigments and their analogs was first recognized long ago in *d*-urobilin and *l*-stercobilin,[9,10] and only many years later was the origin of their intense optical activity explained.[6] Since that time, structure investigations of many diverse tetrapyrrole pigments have shown the considerable utility of chiroptical measurements for determining stereochemistry, as illustrated in

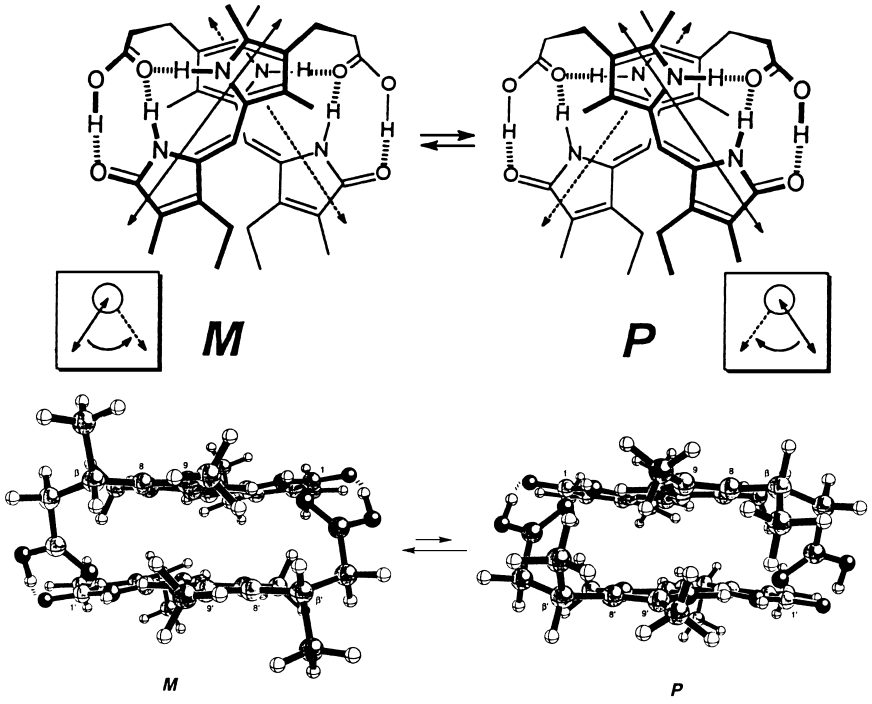

Figure 21. (Upper) Isoenergetic enantiomeric conformations of xanthobilirubic acid interconverting between *M*- and *P*-helicities. The inset boxes show the relative orientations of the dipyrrinones and the long axis-polarized π → π* excitation in their 14π-electron conjugated chromophores. (Lower) Stacked intermolecularly hydrogen-bonded dimers of (β*S*)-methylxanthobilirubic acid (**180**) held in a left-handed (*M*) chiral orientation (left) and in a right-handed (*P*) chiral orientation (right) as viewed from the edge

this review. Dictated by the nature of the UV–vis circular dichroism (or optical rotatory dispersion) method employed, such studies have focussed on the chromophores found in such pigments: either the dipyrrin or dipyrrinone (Section 1). In the former, it is from the helicity of the chromophore imposed by extrachromophoric molecular constraints by which one derives stereochemical information for the molecule. In the latter, it is often from the spatial orientation of two nonconjugated dipyrrinones, as detected by exciton coupling by which one derives stereochemical information for the entire molecule. For linear tetrapyrrole pigments, circular dichroism spectroscopy has thus become an essential tool for 3-dimensional structure investigations in solutions.

Acknowledgements

We are grateful to the National Institutes of Health (HD-17779) for research support, to Mr Michael Huggins for creating the graphics of Figs. 13 and 15, and to Dr. D. Timothy Anstine for creating the graphics used in Fig. 21. Dr. S. E. Boiadjiev is on leave from the Institute of Organic Chemistry, Bulgarian Academy of Sciences.

Appendix A. List of abbreviations

CD, circular dichroism; CE, Cotton effect; DME, dimethyl ester; DMF, dimethyl formamide; DMSO, dimethyl sulfoxide; HMPT, hexamethyl phosphoric triamide; HSA, human serum albumin; ICD, induced circular dichroism; NMR, nuclear magnetic resonance; NOE, nuclear Overhauser effect; ORD, optical rotatory dispersion; P, propionic acid; P^{Me}, propionic acid methyl ester; PPP, Pariser, Pople, Parr; SCF-MO-CI, self-consistent field, molecular orbitals with configuration interaction; TFA, trifluoroacetic acid; TLC, thin layer chromatography; UV, ultraviolet; Vis, visible.

References

1. Falk, H. *The Chemistry of Linear Oligopyrroles and Bile Pigments*. Springer–Verlag: Wien, 1989.
2. Person, R. V.; Peterson, B. R.; Lightner, D. A. *J. Am. Chem. Soc*. **1994**, *116*, 42–59.
3. McDonagh, A. F. Bile pigments: Bilatrienes and 1,15-biladienes. In *The Porphyrins*; Dolphin, D., Ed. Academic Press: New York, 1979; Vol. 6, pp. 293–491.
4. Petryka, Z. J.; Howe, R. B. Historical and clinical aspects of bile pigments. In *The Porphyrins*; Dolphin, D., Ed. Academic Press: New York, 1979; Vol. 6, pp. 805–837.
5. Chowdury, J. R.; Wolkoff, A. W.; Chowdury, N. R.; Arias, I. M. Hereditary jaundice and disorders of bilirubin metabolism. In *The Metabolic and Molecular Bases of Inherited Disease*; Scriver, C. R.; Beaudet, A. L.; Sly, W. S.; Valle, D., Eds. McGraw–Hill: New York, 1995; Vol. II, pp. 2161–2208.
6. Moscowitz, A.; Krueger, W. C.; Kay, I. T.; Skewes, G.; Bruckenstein, S. *Proc. Nat. Acad. Sci. (USA)* **1964**, *52*, 1190–1194.
7. Gray, C. H.; Nicholson, D. C. *J. Chem. Soc*. **1958**, 3085–3099.
8. Watson C. J. *Hoppe Seyler's Z. Physiol. Chem*. **1932**, *204*, 57–67; *ibid*. **1932**, *208*, 101–119; *ibid*. **1933**, *221*, 145–155; *ibid*. **1935**, *233*, 39–58.
9. Fischer, H.; Halbach, H.; Stern, A. *Liebigs Ann. Chem*. **1935**, *519*, 254–260.
10. Schwartz, S.; Watson, C. J. *Proc. Soc. Exp. Biol. Med*. **1942**, *49*, 641–643.
11. Cole, W. J.; Gray, C. H.; Nicholson, D. C. *J. Chem. Soc*. **1965**, 4085–4091.
12. Lowry, P. T.; Cardinal, R.; Collins, S.; Watson, C. J. *J. Biol. Chem*. **1956**, *218*, 641–646.
13. Gray, C. H.; Jones, P. M.; Klyne, W.; Nicholson, D. C. *Nature*, **1959**, *184*, 41–42.
14. Moscowitz, A. *Adv. Chem. Phys*. **1962**, *4*, 67–112.
15. Deutsche, C. W.; Lightner, D. A.; Woody, R. W.; Moscowitz, A. *Annual Review of Physical Chemistry* **1969**, *20*, 407–448.
16. Moscowitz, A. *Proc. Royal Soc. London, Ser. A*, **1967**, *297*, 16–26.
17. Cole, W. J.; Gray, C. H.; Nicholson, D. C.; Norman, M. *J. Chem. Soc. (C)* **1966**, 1321–1326.
18. Lightner, D. A.; Docks, E. L.; Horwitz, J.; Moscowitz, A. *Proc. Nat. Acad. Sci. (USA)* **1970**, *67*, 1361–1366.
19. Plieninger, H.; Lerch, U. *Liebigs Ann. Chem*. **1966**, *698*, 196–208.
20. Plieninger, H.; Ruppert, J. *Liebigs Ann. Chem*. **1970**, *736*, 43–61.
21. Brockmann Jr., H.; Knobloch, G.; Plieninger, H.; Ehl, K.; Ruppert, J.; Moscowitz, A.; Watson, C. J. *Proc. Nat. Acad. Sci. (USA)* **1971**, *68*, 2141–2144.
22. Plieninger, H.; Ehl, K.; Tapia, A. *Liebigs Ann. Chem*. **1970**, *736*, 62–67.
23. Gossauer, A.; Weller, J.-P. *Chem. Ber*. **1978**, *111*, 486–501.
24. Pasquier, C.; Gossauer, A.; Keller, W.; Kratky, C. *Helv. Chim. Acta* **1987**, *70*, 2098–2109.
25. Gossauer, A.; Fehr, F. Nydegger, F.; Stöckli-Evans, H. *J. Am. Chem. Soc*. **1997**, *119*, 1599–1608.
26. Lightner, D. A.; Hefelfinger, D. T.; Powers, T. W.; Frank. G. W.; Trueblood, K. N. *J. Am. Chem. Soc*. **1972**, *94*, 3492–3497.
27. Flock, L.; Nydegger, F.; Gossauer, A.; Kratky, C. *Helv. Chim. Acta* **1994**, *77*, 445–452.
28. Snatzke, G. *Angew. Chem., Int. Ed. Engl*. **1979**, *18*, 363–377.
29. Schippers, P. H.; Dekkers, H. P. J. M. *J. Am. Chem. Soc*. **1983**, *105*, 79–84.
30. Sheldrick, W. S. *J. Chem. Soc., Perkin Trans. 2* **1976**, 1457–1462.
31. Wagner, U.; Kratky, C.; Falk, H.; Wöss, H. *Monatsh. Chem*. **1991**, *122*, 749–758.
32. Lehner, H.; Riemer, W.; Schaffner, K. *Liebigs Ann. Chem*. **1979**, 1798–1801.
33. Manitto, P.; Monti, D. *J. Chem. Soc., Chem. Commun*. **1976**, 122–123.
34. Blauer, G.; Wagnière, G. *J. Am. Chem. Soc*. **1975**, *97*, 1949–1954.
35. Wagnière, G.; Blauer, G. *J. Am. Chem. Soc*. **1976**, *98*, 7806–7810.

36. Falk, H.; Thirring, K. *Tetrahedron* **1981**, *37*, 761–766.
37. Moscowitz, A. *Tetrahedron* **1961**, *13*, 48–56.
38. Hug, W.; Wagnière, G. *Tetrahedron* **1972**, *28*, 1241–1248.
39. Haidl, E.; Krois, D.; Lehner, H. *J. Chem. Soc., Perkin Trans. 2* **1985**, 421–425.
40. Krois, D.; Lehner, H. *Monatsh. Chem*. **1986**, *117*, 1205–1217.
41. Krois, D.; Lehner, H. *J. Chem. Soc., Perkin Trans. 2* **1987**, 219–225.
42. Krois, D.; Lehner, H. *J. Chem. Soc., Perkin Trans. 2* **1987**, 1523–1526.
43. Haidl, E.; Krois, D.; Lehner, H. *Monatsh. Chem*. **1985**, *116*, 119–131.
44. Krois, D.; Lehner, H. *J. Chem. Soc., Perkin Trans. 2* **1990**, 1745–1755; Corrigendum *ibid*. **1991**, 437.
45. Krois, D.; Lehner, H. *Monatsh. Chem*. **1991**, *122*, 89–100.
46. Huber, R.; Schneider, M.; Mayr, I.; Müller, R.; Deutzmann, R.; Suter, F.; Zuber, H.; Falk, H.; Kayser, H. *J. Mol. Biol*. **1987**, *198*, 499–513.
47. Scheer, H.; Kayser, H. *Z. Naturforsch*. **1988**, *43C*, 84–90.
48. Wagner, U. G.; Müller, N.; Schmitzberger, W.; Falk, H.; Kratky, C. *J. Mol. Biol*. **1995**, *247*, 326–337.
49. Falk, H.; Marko, H.; Müller, N.; Schmitzberger, W.; Stumpe, H. *Monatsh. Chem*. **1990**, *121*, 893–901.
50. Krois, D.; Lehner, H. *J. Chem. Soc., Perkin Trans. 1* **1989**, 2179–2185.
51. Krois, D.; Lehner, H. *Monatsh. Chem*. **1989**, *120*, 789–795.
52. Krois, D.; Lehner, H. *J. Chem. Soc., Perkin Trans. 2* **1993**, 1351–1360.
53. Krois, D.; Lehner, H. *J. Chem. Soc., Perkin Trans. 2* **1989**, 2085–2090.
54. Krois, D. *Monatsh. Chem*. **1991**, *122*, 495–506.
55. Krois, D.; Lehner, H. *J. Chem. Soc., Perkin Trans. 2* **1993**, 1837–1840.
56. Boiadjiev, S. E.; Anstine, D. T.; Lightner, D. A. *Tetrahedron: Asymmetry* **1995**, *6*, 901–912.
57. Scheer, H. *Angew. Chem., Int. Ed. Engl*. **1981**, *20*, 241–261.
58. Gossauer, A. *Tetrahedron* **1983**, *39*, 1933–1941.
59. Cole, W. J.; Ó hEocha, C.; Moscowitz, A.; Krueger, W. R. *Eur. J. Biochem*. **1967**, *3*, 202–207.
60. Brockmann Jr., H.; Knobloch, G. *Chem. Ber*. **1973**, *106*, 803–811.
61. Klein, G.; Rüdiger, W. *Liebigs Ann. Chem*. **1978**, 267–279.
62. Gossauer, A.; Weller, J.-P. *J. Am. Chem. Soc*. **1978**, *100*, 5928–5933.
63. Lagarias, J. C.; Glazer, A. N.; Rapoport, H. *J. Am. Chem. Soc*. **1979**, *101*, 5030–5037.
64. Schoch, S.; Klein, G.; Linsenmeier, U.; Rüdiger, W. *Liebigs Ann. Chem*. **1976**, 549–558.
65. Schoenleber, R. W.; Kim, Y.; Rapoport, H. *J. Am. Chem. Soc*. **1984**, *106*, 2645–2651.
66. Schoenleber, R. W.; Leung, S.-L.; Lundell, D. J.; Glazer, A. N.; Rapoport, H. *J. Am. Chem. Soc*. **1983**, *105*, 4072–4076.
67. Lagarias, J. C.; Rapoport, H. *J. Am. Chem. Soc*. **1980**, *102*, 4821–4828.
68. Grubmayr, K.; Widhalm, M. *Monatsh. Chem*. **1987**, *118*, 837–843.
69. Falk, H.; Kapl, G.; Medinger, W. *Monatsh. Chem*. **1985**, *116*, 1065–1085.
70. Edinger, J.; Falk, H.; Jungwirth, W.; Müller, N.; Zrunek, U. *Monatsh. Chem*. **1984**, *115*, 1081–1099.
71. Edinger, J.; Falk, H.; Müller, N. *Monatsh. Chem*. **1984**, *115*, 837–852.
72. Cheng, L.; Jiang, L. *J. Photochem. Photobiol. B: Biol*. **1992**, *15*, 343–353.
73. Micura, R.; Grubmayr, K. *Angew. Chem., Int. Ed. Engl*. **1995**, *34*, 1733–1735.
74. Stanek, M.; Grubmayr, K. *Chem. Eur. J*. **1998**, *4*, 1653–1659.
75. Stanek, M.; Grubmayr, K. *Chem. Eur. J*. **1998**, *4*, 1660–1666.
76. Falk, H.; Kapl, G.; Medinger, W.; Müller, N. *Monatsh. Chem*. **1987**, *118*, 973–985.
77. Falk, H.; Medinger, W.; Müller, N. *Monatsh. Chem*. **1988**, *119*, 113–126.
78. Blauer, G. *Israel J. Chem*. **1983**, *23*, 201–209.
79. Scharnagl, C.; Köst-Reyes, E.; Scheider, S.; Köst, H.-P.; Scheer, H. *Z. Naturforsch*. **1983**, *38C*, 951–959.
80. Schneider, S.; Köst-Reyes, E.; Scharnagl, C.; Geiselhart, P. *Photochem. Photobiol*. **1986**, *44*, 771–777.
81. Bishop, J. E.; Rapoport, H.; Klotz, A. V.; Chan, C. F.; Glazer, A. N.; Füglistaller, P.; Zuber, H. *J. Am. Chem. Soc*. **1987**, *109*, 875–881.
82. Bishop, J. E.; Lagarias, J. C.; Nagy, J. O.; Schoenleber, R. W.; Rapoport, H.; Klotz, A. V.; Glazer, A. N. *J. Biol. Chem*. **1986**, *261*, 6790–6796.
83. Klotz, A. V.; Glazer, A. N.; Bishop, J. E.; Nagy, J. O.; Rapoport, H. *J. Biol. Chem*. **1986**, *261*, 6797–6805.
84. Schirmer, T.; Bode, W.; Huber, R. *J. Mol. Biol*. **1987**, *196*, 677–695.
85. Mimuro, M.; Rümbeli, R.; Füglistaller, P.; Zuber, H. *Biochim. Biophys. Acta* **1986**, *851*, 447–456.
86. Siebzehnrübl, S.; Fischer, R.; Scheer, H. *Z. Naturforsch*. **1987**, *42C*, 258–262.

87. Scharnagl, C.; Schneider, S. *J. Photochem. Photobiol. B: Biol*. **1989**, *3*, 603–614.
88. Scharnagl, C.; Köst-Reyes, E.; Schneider, S. In *Optical Properties and Structure of Tetrapyrroles*; Blauer, G.; Sund, H., Eds. Walter de Gruyter: Berlin, 1985; pp. 394–410.
89. Scharnagl, C.; Schneider, S. *J. Photochem. Photobiol. B: Biol*. **1991**, *8*, 129–157.
90. MacColl, R.; Lam, I.; Choi, C. Y.; Kim, J. *J. Biol. Chem*. **1994**, *269*, 25465–25469.
91. (a) Siebzehnrübl, S.; Fischer, R.; Kufer, W.; Scheer, H. *Photochem. Photobiol*. **1989**, *49*, 753–761; (b) Kufer, W.; Björn, G. S. *Physiol. Plant*. **1989**, *75*, 389–394; (c) Maruthi Sai, P. S.; Siebzehnrübl, S.; Mahajan, S.; Scheer, H. *Photochem. Photobiol*. **1992**, *55*, 119–124.
92. Maruthi Sai, P. S.; Siebzehnrübl, S.; Mahajan, S.; Scheer, H. *Photochem. Photobiol*. **1993**, *57*, 71–75.
93. (a) Rüdiger, W.; Thümmler, F. In *Photomorphogenesis in Plants*, 2nd Edition; Kendrick, R. E.; Kronenberg, G. H. M., Eds. Kluwer: Dordrecht, The Netherlands, 1994; pp. 51–69; (b) Rüdiger, W.; Thümmler, F. *Angew. Chem., Int. Ed. Engl*. **1991**, *30*, 1216–1228; (c) Eilfeld, P.; Haupt, W. In *Photoreceptor Evolution and Function*; Holmes, M. G., Ed. Academic Press: London, 1991; pp. 203–239.
94. Thümmler, F.; Rüdiger, W. *Tetrahedron* **1983**, *39*, 1943–1951.
95. (a) Vierstra, R. D.; Quail, P. H.; Hahn, T.-R.; Song, P.-S. *Photochem. Photobiol*. **1987**, *45*, 429–432; (b) Sommer, D.; Song, P.-S. *Biochemistry* **1990**, *29* 1943–1948 (c) Chai, Y.-G.; Song, P.-S.; Gordonnier, M.-M.; Pratt, L. H. *Biochemistry* **1987**, *26*, 4947–4952.
96. Burke, M. J.; Pratt, D. C.; Moscowitz, A. *Biochemistry* **1972**, *11*, 4025–4031.
97. Thümmler, F.; Rüdiger, W. *Israel J. Chem*. **1983**, *23*, 195–200.
98. (a) Kohen, E.; Santus, R.; Hirschberg, J. G. *Photobiology*; Acad. Press: San Diego, CA, 1995; pp. 227–257; (b) Rospendowski, B. N.; Farrens, D. L.; Cotton, T. M.; Song, P.-S. *FEBS Lett*. **1989**, *258*, 1–4.
99. Zhang, C.-F.; Farrens, D. L.; Björling, S. C.; Song, P.-S., Kliger, D. S. *J. Am. Chem. Soc*. **1992**, *114*, 4569–4580.
100. Eilfeld, P. H.; Eilfeld, P. G. *Physiol. Plant*. **1988**, *74*, 169–175.
101. Björling, S. C.; Zhang, C.-F.; Farrens, D. L.; Song, P.-S.; Kliger, D. S. *J. Am. Chem. Soc*. **1992**, *114*, 4581–4588.
102. Chen, E.; Parker, W.; Lewis, J. W.; Song, P.-S.; Kliger, D. S. *J. Am. Chem. Soc*. **1993**, *115*, 9854–9855.
103. Mühlecker, W.; Ongania, K.-H.; Kräutler, B.; Matile, P.; Hörtensteiner, S. *Angew. Chem., Int. Ed. Engl*. **1997**, *36*, 401–404.
104. (a) McDonagh, A. F.; Lightner, D. A. In *Hepatic Metabolism and Disposition of Endo and Xenobiotics*, Falk Symposium No. 57; Bock, K. W.; Gerok, W.; Matern, S., Eds. Kluwer: Dordrecht, The Netherlands, 1991; Chap. 5, pp. 47–59; (b) McDonagh, A. F.; Lightner, D. A. *Cellular and Molecular Biology* **1994**, *40*, 965–974.
105. (a) McDonagh, A. F.; Lightner, D. A. *Pediatrics* **1985**, *75*, 443–455; (b) Lightner, D. A.; McDonagh, A. F. *Accounts Chem. Res*. **1984**, *17*, 417–424.
106. Fischer, H.; Plieninger, H.; Weissbarth, O. *Hoppe-Seyler's Z. Physiol. Chem*. **1941**, *268*, 197–226.
107. (a) Bonnett, R.; Davies, J. E.; Hursthouse, M. B. *Nature* **1976**, *262*, 326–328. (b) Bonnett, R.; Davies, J. E.; Hursthouse, M. B.; Sheldrick, G. M. *Proc. Royal Soc., London Ser. B* **1978**, *B202*, 249–268.
108. LeBas, G.; Allegret, A.; Mauguen, Y.; DeRango, C.; Bailly, M. *Acta Crystallogr*. **1980**, *B36*, 3007–3011.
109. (a) Mugnoli, A.; Manitto, P.; Monti, D. *Nature* **1978**, *273*, 568–569; (b) Mugnoli, A.; Manitto, P.; Monti, D. *Acta Crystallogr*. **1983**, *C39*, 1287–1291.
110. Becker, W.; Sheldrick, W. S. *Acta Crystallogr*. **1978**, *B34*, 1298–1304.
111. Knell, A. J.; Hancock, F.; Hutchinson, D. W. In *Metabolism and Chemistry of Bilirubin and Related Tetrapyrroles*; Bakken, A. F.; Fog, J., Eds. Pediatric Research Institute: Oslo, 1975; p. 234.
112. Kuenzle, C. C.; Weibel, M. H.; Pelloni, R. R.; Hemmerich, P. *Biochem. J*. **1973**, *133*, 364–368.
113. Navon, G.; Frank, S.; Kaplan, D. *J. Chem. Soc., Perkin Trans. 2* **1984**, 1145–1149.
114. Boiadjiev, S. E.; Holmes, D. L.; Anstine, D. T.; Lightner, D. A. *Tetrahedron* **1995**, *51*, 10663–10678.
115. Kuenzle, C. C.; Gitzelmann-Gumarasamy, N.; Wilson, K. J. *J. Biol. Chem*. **1976**, *251*, 801–807.
116. Lightner, D. A.; Zhang, M.-H. *Tetrahedron* **1988**, *44*, 4679–4688.
117. Lightner, D. A.; Gawronski, J. K.; Wijekoon, W. M. D. *J. Am. Chem. Soc*. **1987**, *109*, 6354–6362.
118. Kasha, M.; Rawls, H. R.; El-Bayoumi, M. A. *Pure Appl. Chem*. **1965**, *32*, 371–392.
119. Harada, N.; Nakanishi, K. Circular Dichroism Spectroscopy — Exciton Coupling in Organic Stereochemistry. Univ. Sci. Books: Mill Valley, CA, 1983.
120. Falk, H.; Grubmayr, K.; Höllbacher, G.; Hofer, O.; Leodolter, A.; Neufingerl, F.; Ribò, J. M. *Monatsh. Chem*. **1977**, *108*, 1113–1130.
121. Lightner, D. A.; Zhang, M.-H.; Trull, F. R. *Tetrahedron Lett*. **1987**, *28*, 4033–4036.
122. Lightner, D. A.; Zhang, M.-H. *Spectroscopy Lett*. **1988**, *21*, 469–480.
123. Lightner, D. A.; McDonagh, A. F.; Wijekoon, W. M. D.; Reisinger, M. *Tetrahedron Lett*. **1988**, *29*, 3507–3510.

124. Lightner, D. A.; Person, R.; Peterson, B.; Puzicha, G.; Pu, Y.-M.; Boiadjiev, S. E. Biomolecular Spectroscopy II; Birge, R.; Nafie, L., Eds. *Proc. SPIE-Int. Soc. Opt. Eng*. **1991**, *1432*, 2–13.
125. Puzicha, G.; Pu, Y.-P.; Lightner, D. A. *J. Am. Chem. Soc*. **1991**, *113*, 3583–3592.
126. Lightner, D. A.; Wijekoon, W. M. D.; Zhang, M.-H. *J. Biol. Chem*. **1988**, *263*, 16669–16676.
127. Boiadjiev, S. E.; Lightner, D. A. *Tetrahedron: Asymmetry* **1997**, *8*, 2115–2129.
128. Boiadjiev, S. E.; Person, R. V.; Puzicha, G.; Knobler, C.; Maverick, E.; Trueblood, K. N.; Lightner, D. A. *J. Am. Chem. Soc*. **1992**, *114*, 10123–10133.
129. Pu, Y.-M.; Lightner, D. A. *Spectroscopy Lett*. **1991**, *24*, 983–993.
130. Boiadjiev, S. E.; Anstine, D. T.; Lightner, D. A. *Tetrahedron: Asymmetry* **1994**, *5*, 1945–1964.
131. Pu, Y.-M.; Lightner, D. A. *Tetrahedron* **1991**, *47*, 6163–6170.
132. Boiadjiev, S. E.; Person, R. V.; Lightner, D. A. *Tetrahedron: Asymmetry* **1993**, *4*, 491–510.
133. Boiadjiev, S. E.; Lightner, D. A. *Chirality* **1997**, *9*, 604–615.
134. Boiadjiev, S. E.; Anstine, D. T.; Maverick, E.; Lightner, D. A. *Tetrahedron: Asymmetry* **1995**, *6*, 2253–2270.
135. Boiadjiev, S. E.; Lightner, D. A. *Tetrahedron: Asymmetry* **1996**, *7*, 1309–1322.
136. Boiadjiev, S. E.; Lightner, D. A. *Tetrahedron: Asymmetry* **1997**, *8*, 3603–3615.
137. Boiadjiev, S. E.; Pfeiffer, W. P.; Lightner, D. A. *Tetrahedron* **1997**, *53*, 14547–14564.
138. Falk, H.; Marko, H.; Müller, N., Schmitzberger, W. *Monatsh. Chem*. **1990**, *121*, 903–908.
139. Byun, Y.-S.; Lightner, D. A. *J. Org. Chem*. **1991**, *56*, 6027–6033.
140. Lightner, D. A.; Reisinger, M.; Wijekoon, W. M. D. *J. Org. Chem*. **1987**, *52*, 5391–5395.
141. Boiadjiev, S. E.; Anstine, D. T.; Lightner, D. A. *J. Am. Chem. Soc*. **1995**, *117*, 8727–8736.